

# Proton radiography in proton therapy treatment

**Aleksandra K. Biegun**

4-9 June 2017, Cracow, Poland

[a.k.biegun@rug.nl](mailto:a.k.biegun@rug.nl)



university of  
 groningen

kvi - center for advanced  
 radiation technology

A.K. Biegun  
E.R. van der Graaf  
S. Brandenburg



umcg

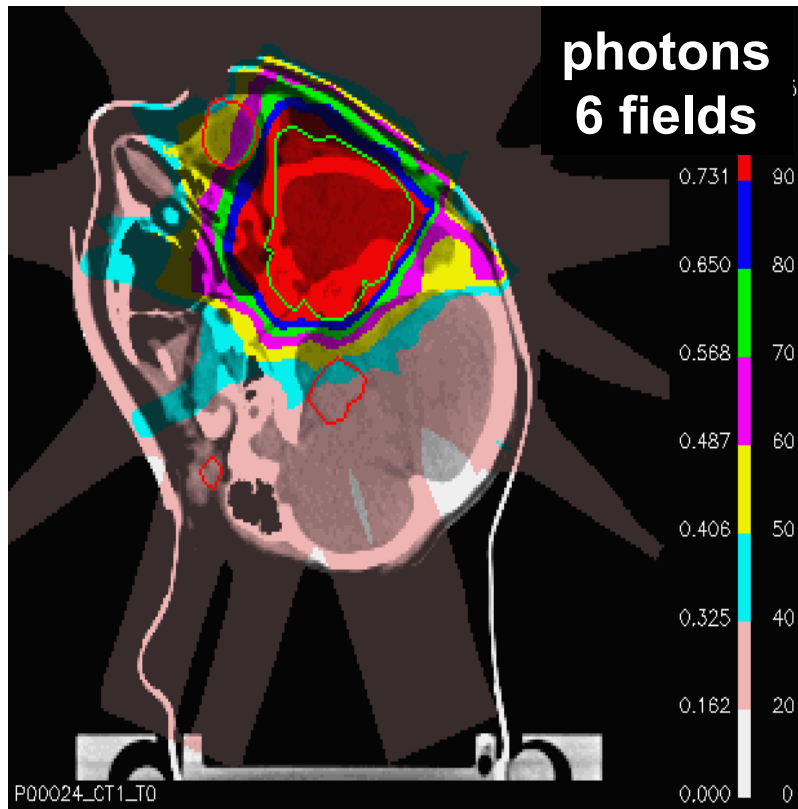
M-J. van Goethem



J. Visser  
M. van Beuzekom  
E.N. Koffeman

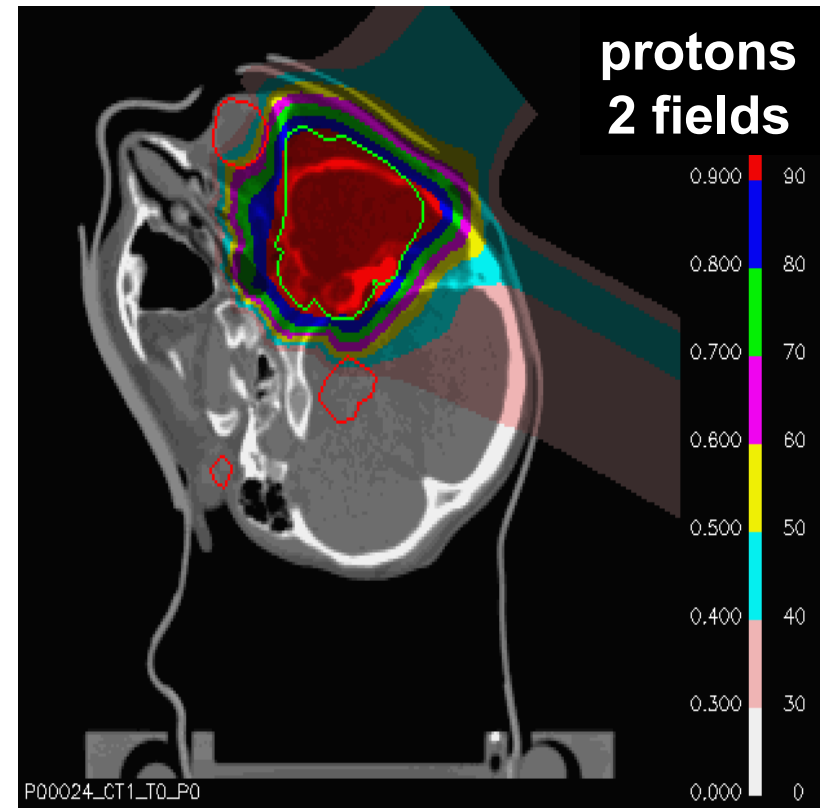
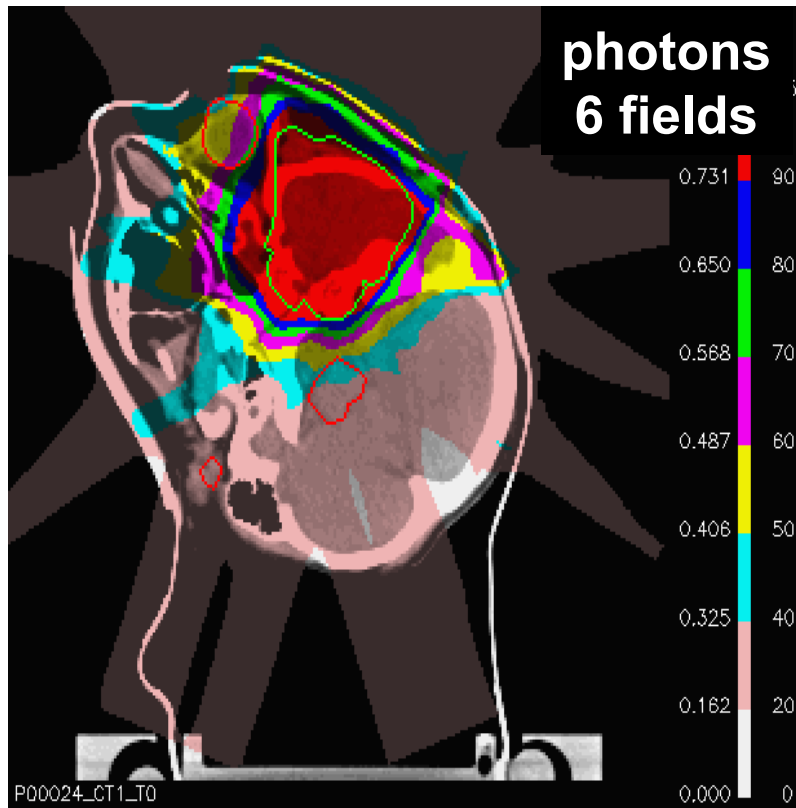
# Photons vs. protons

source: T. Lomax, PSI



# Photons vs. protons

source: T. Lomax, PSI



**Integral dose to healthy tissue for protons is 6 times lower!**

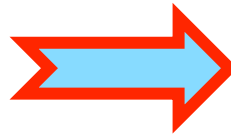
# Proton therapy work flow

## CT scan



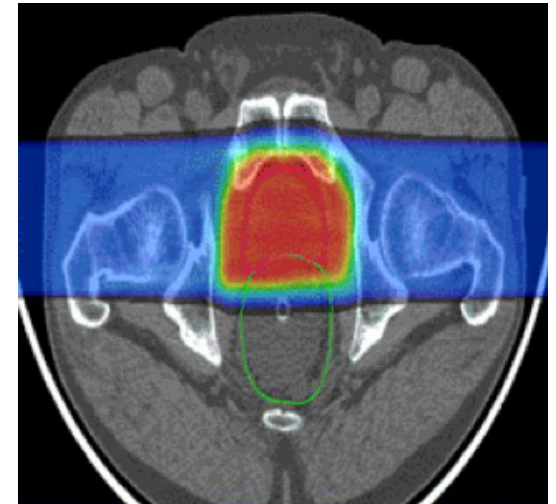
$$HU = 1000 \frac{\mu - \mu_{water}}{\mu_{water}}$$

Translation

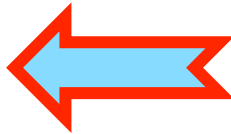


3D map of proton  
 stopping powers (PSP)

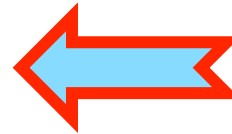
Treatment  
 planning



Treatment  
 verification



Treatment





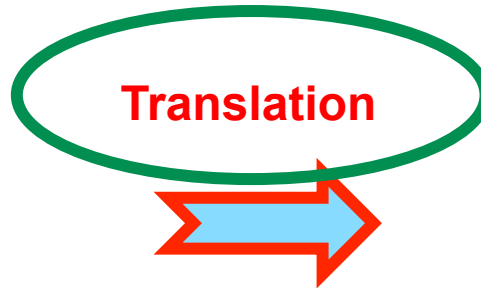
# Proton therapy work flow

CT scan



$$HU = 1000 \frac{\mu - \mu_{water}}{\mu_{water}}$$

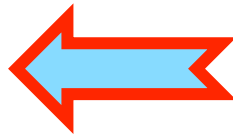
Knowledge of patient



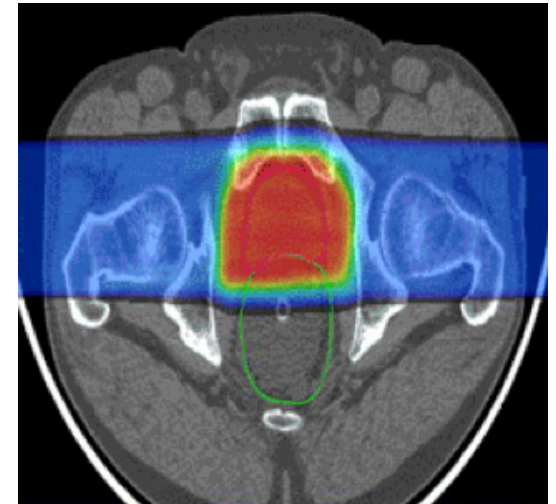
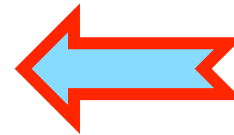
3D map of proton  
 stopping powers (PSP)



Treatment  
 verification



Treatment



# Knowledge of patient in proton therapy treatment

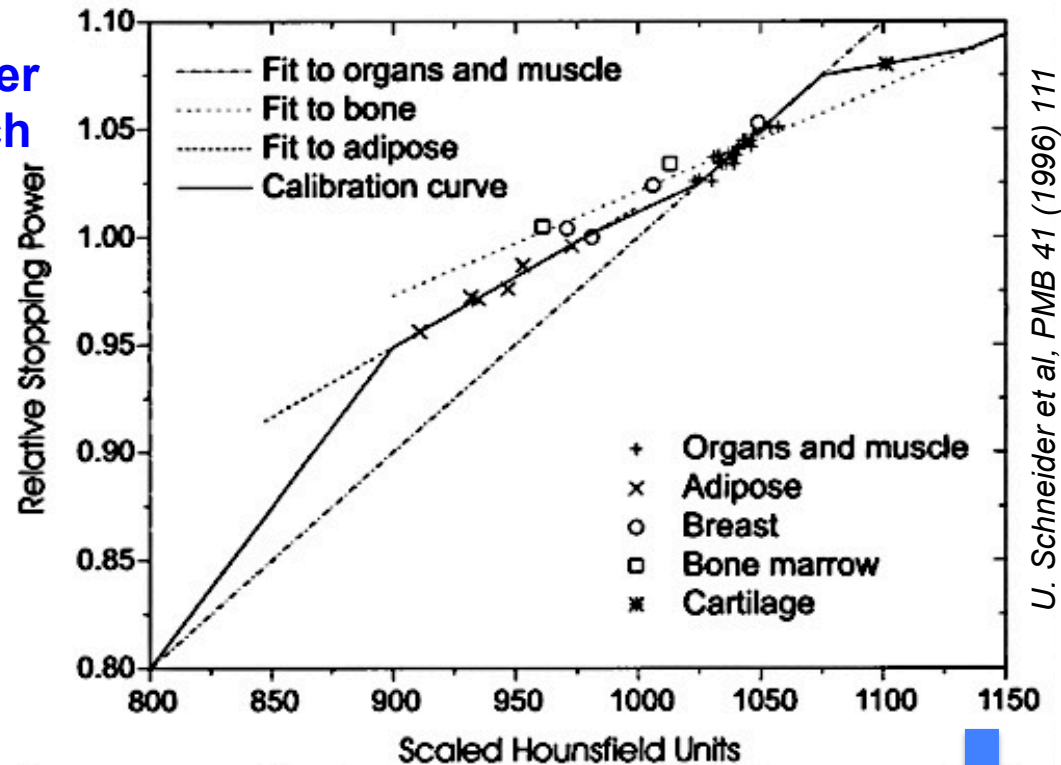
## CT scan



Schneider  
approach



$$HU = 1000 \frac{\mu - \mu_{water}}{\mu_{water}}$$



3D map of proton  
stopping powers



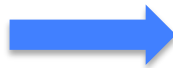
- Conversion HU to stopping power is NOT unique
- Systematic uncertainties of 3-4% require larger than necessary irradiation safety margins around the tumor

# ... And the consequence...

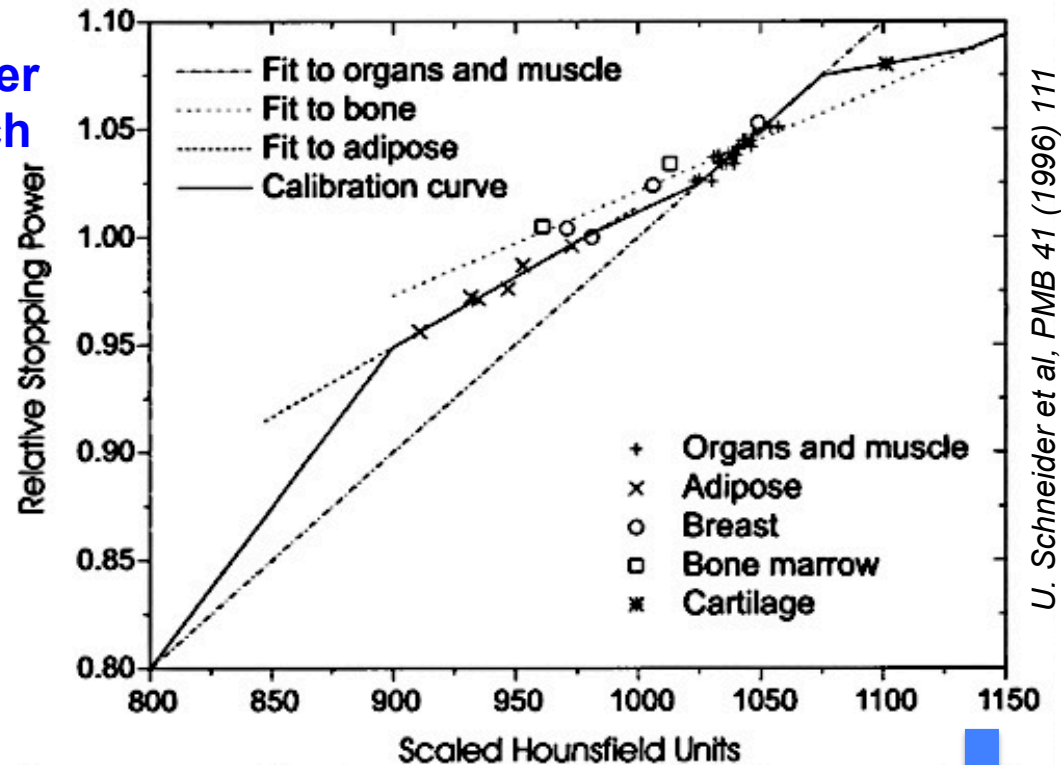
## CT scan



Schneider  
approach



$$HU = 1000 \frac{\mu - \mu_{water}}{\mu_{water}}$$



- Conversion HU to stopping power is NOT unique
- Systematic uncertainties of 3-4% require larger than necessary irradiation safety margins around the tumor

3D map of proton  
stopping powers

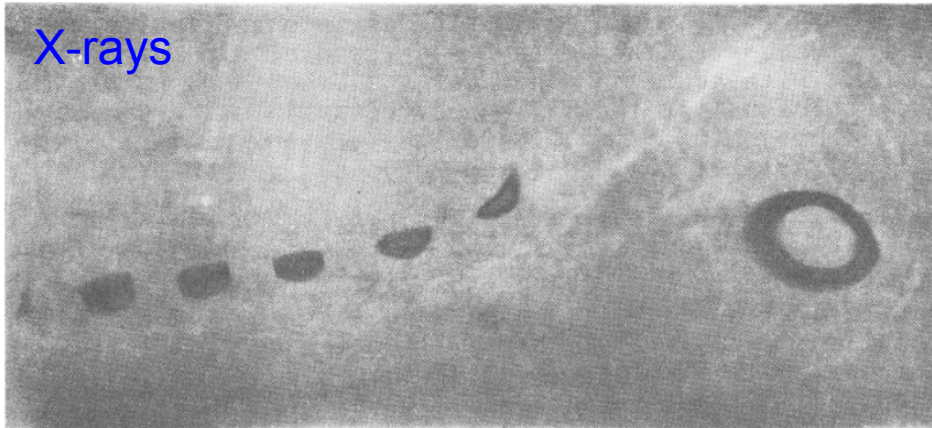
Leads to increased dose  
in healthy tissues



# Why proton radiography?

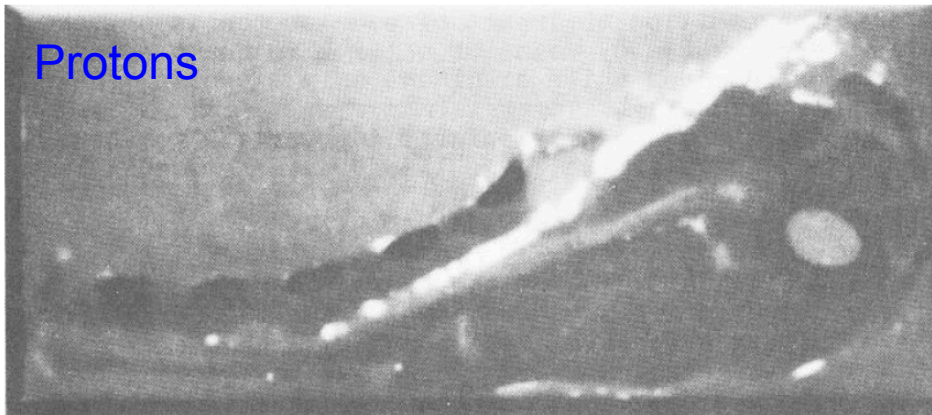
- ✧ A lamb chop 1 cm thick immersed in 12.5 cm thick water phantom
- ✧  $E_{\text{X-rays}} = 30 \text{ kVp}$
- ✧  $E_{\text{p}} = 160 \text{ MeV}$

X-rays



- (-) much less contrast for fat
- (-) no contrast for lean meat (muscle)
- (+) much better spatial resolution

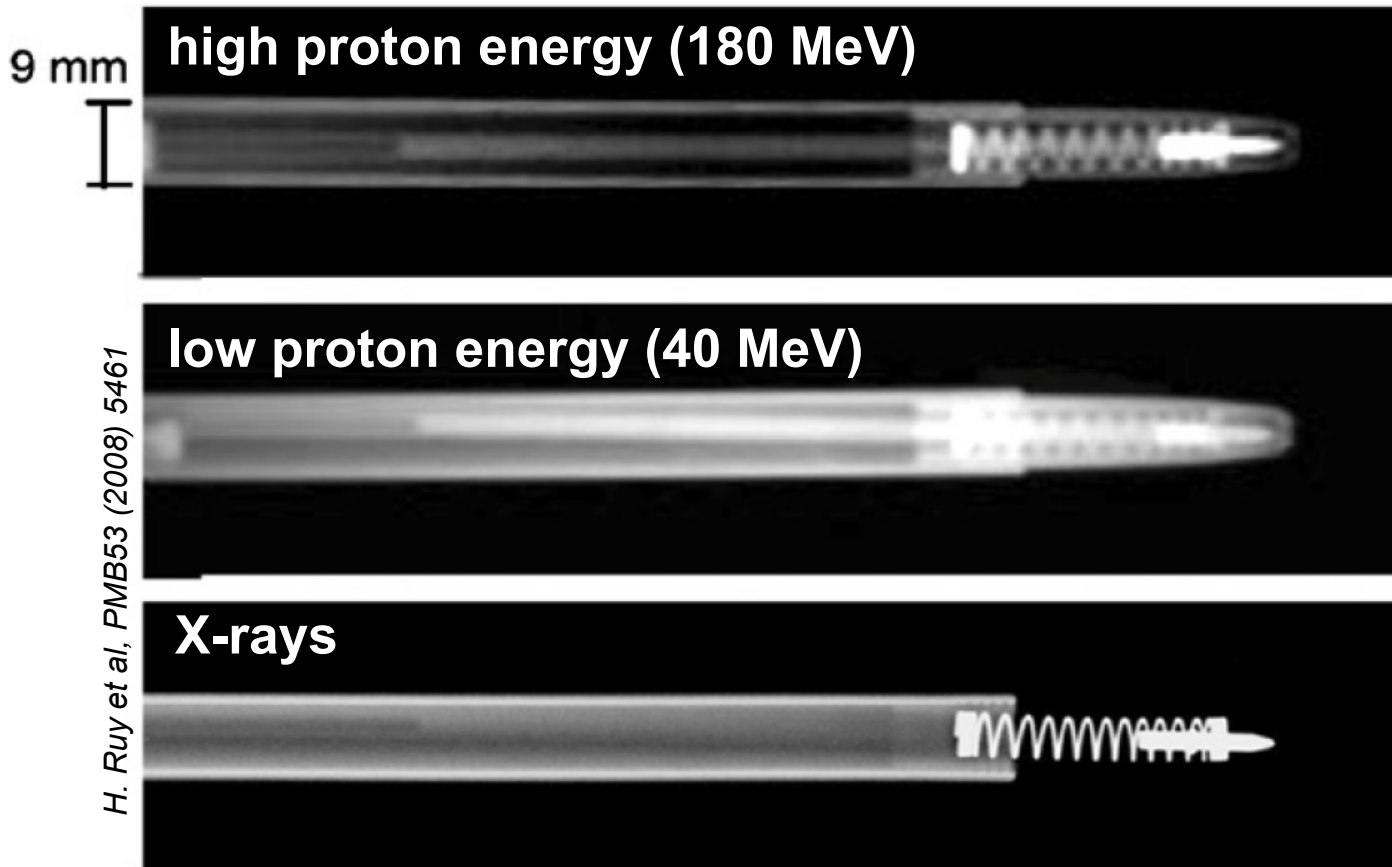
Protons



- (-) poor spatial resolution
- (+) high contrast for soft tissues

# Why proton radiography?

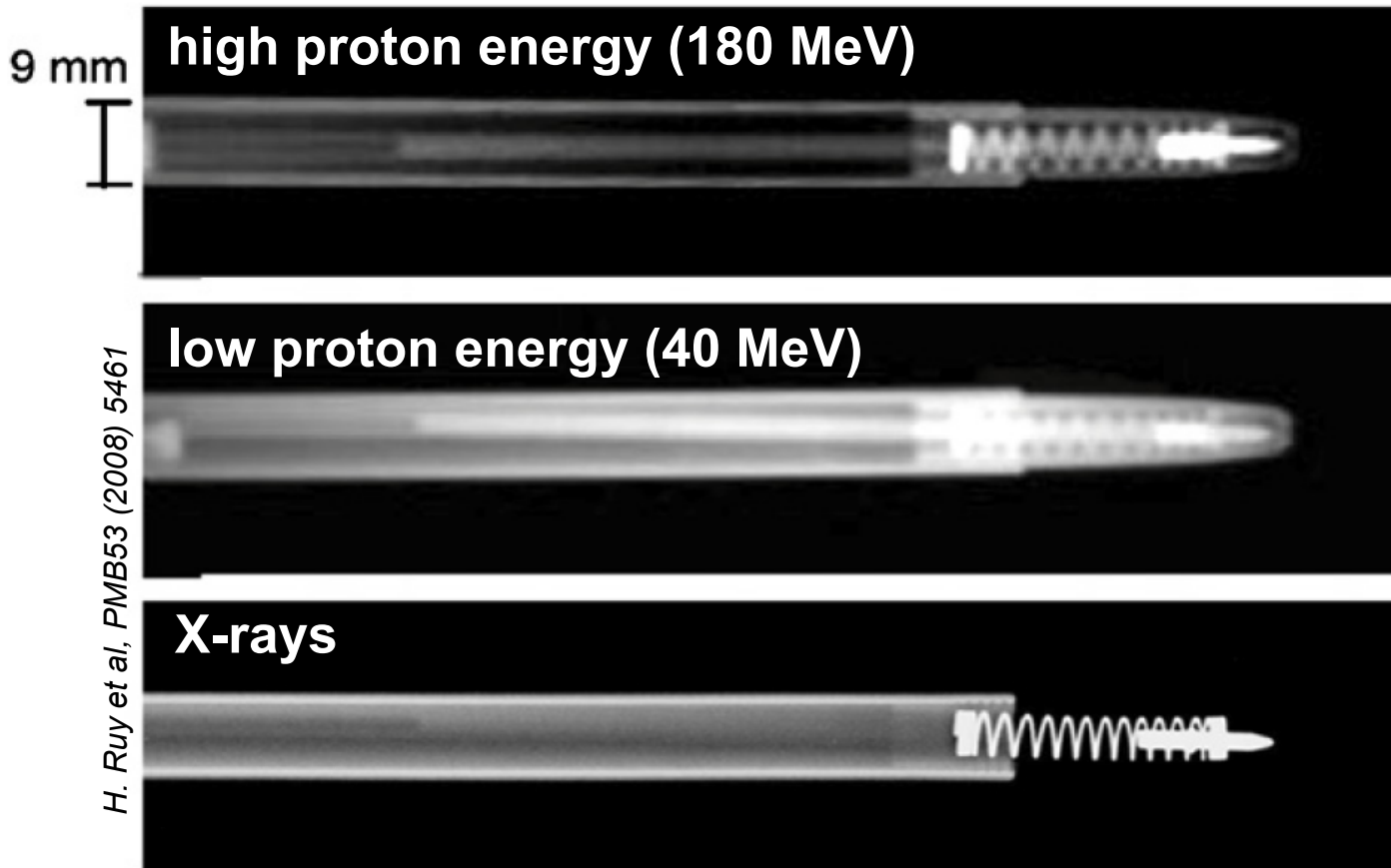
- ✧ High resolving power for proton beam (centerpiece of the pen visible)
- ✧ X-ray produces a clearer image of the spring, but density resolution for the centerpiece is not high





# Why proton radiography?

- ✧ High resolving power for proton beam (centerpiece of the pen visible)
- ✧ X-ray produces a clearer image of the spring, but density resolution for the centerpiece is not high



Protons  
 help  
 to improve  
 determination  
 of energy losses  
 in “soft material”

## ✧ Advantage:



Proton stopping powers measured directly



Decrease uncertainty of Relative PSP (RPSP)  
 derived from stoichiometric calibration with X-ray CT



Optimize treatment plan for the patient

## ✧ Challenge:

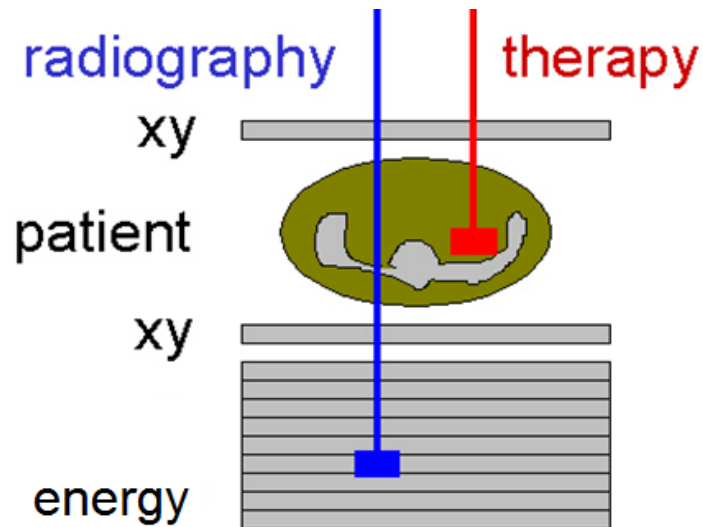


Proton undergoes multiple Coulomb scattering causing image blurring



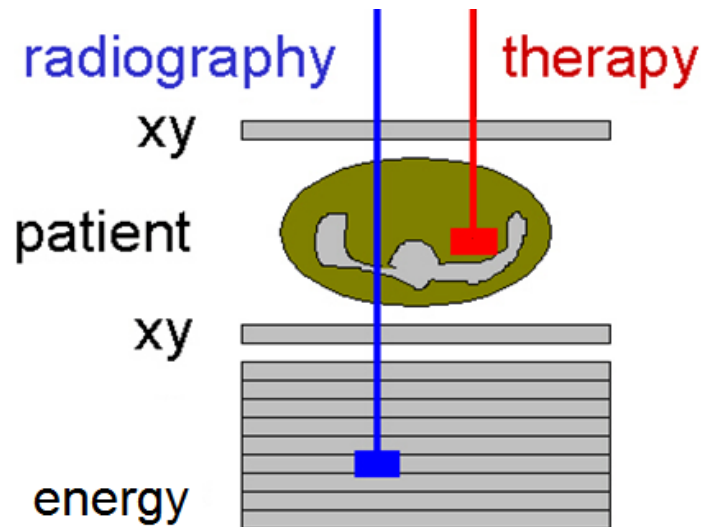
# What is proton radiography?

- ✧ Proton beam energy higher than the therapeutic energies, i.e. protons pass through the patient



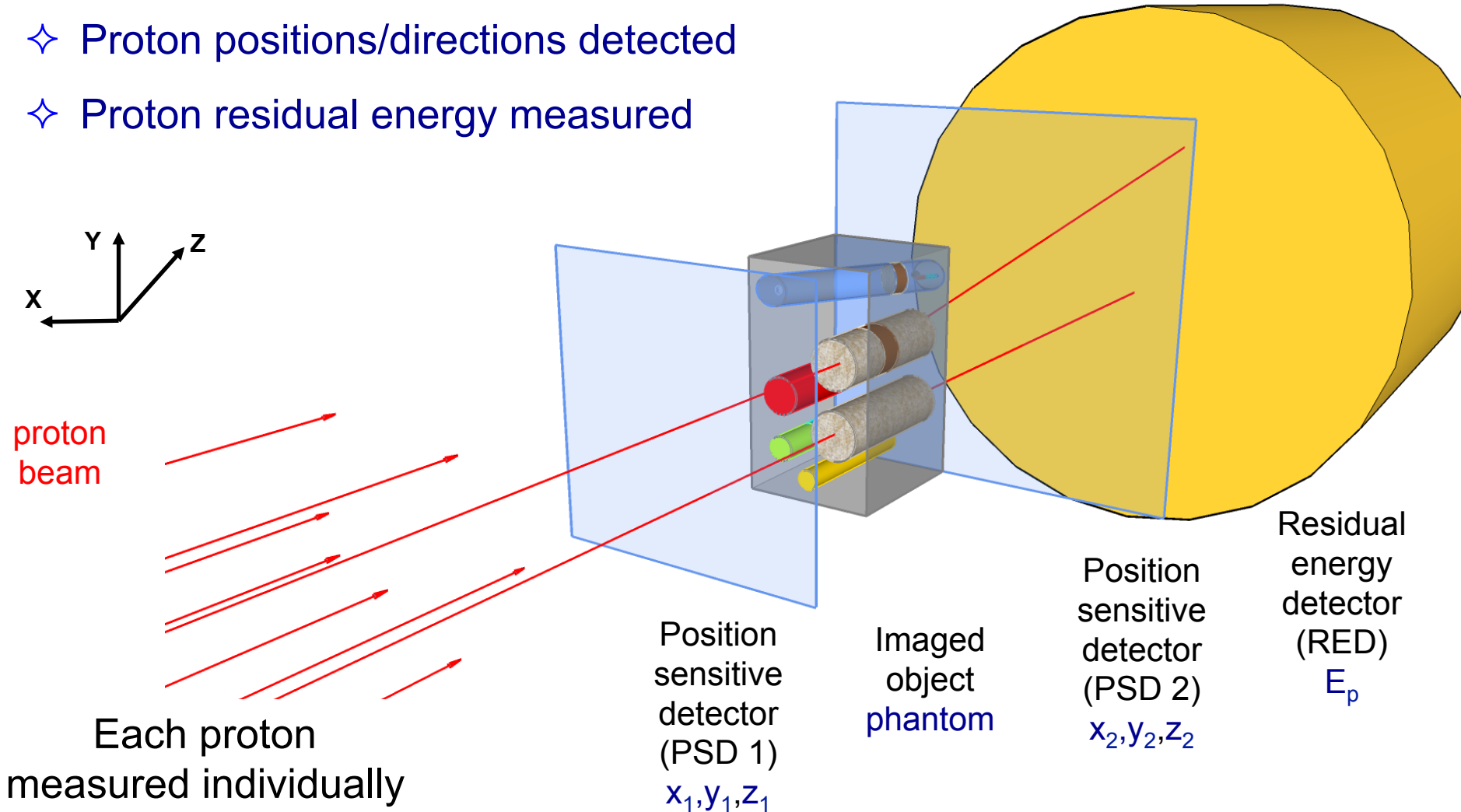
# What is proton radiography?

- ✧ Proton beam energy higher than the therapeutic energies, i.e. protons pass through the patient
- ✧ Position sensitive detectors: before and after the patient
- ✧ Range / residual energy detector: after the patient



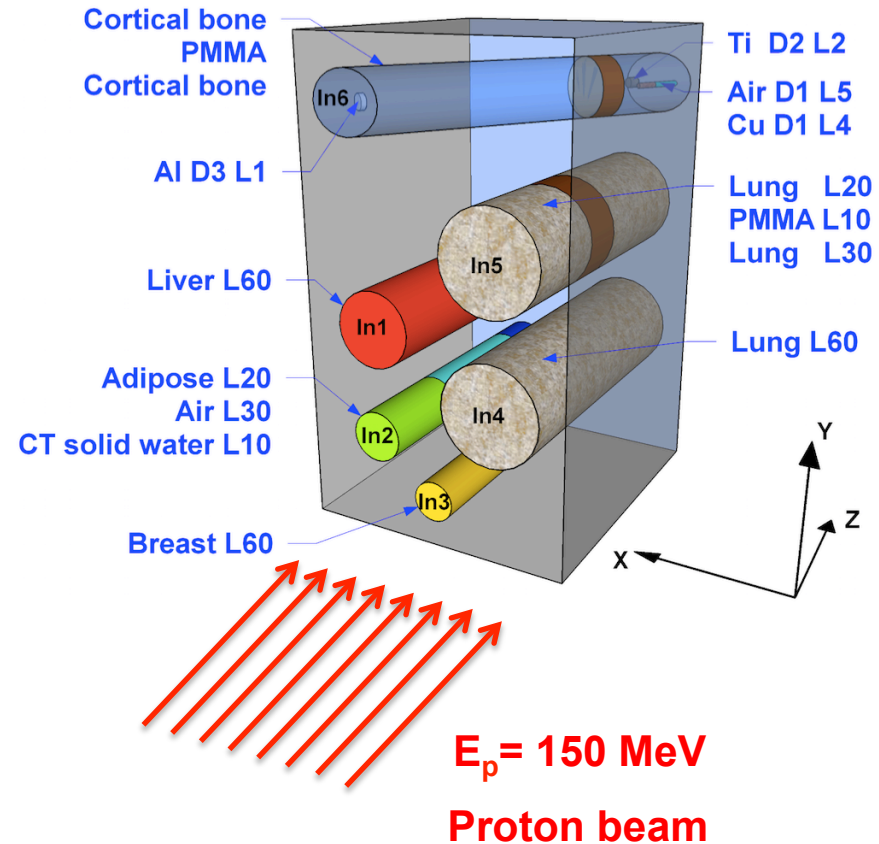
# Proton radiography: Geant4 MC simulations

- ✧  $50 \cdot 10^6$  protons generated, scattered beam,  $E_p = 150$  MeV
- ✧ Proton positions/directions detected
- ✧ Proton residual energy measured



# Complex phantom (54 x 94 x 60 mm<sup>3</sup>)

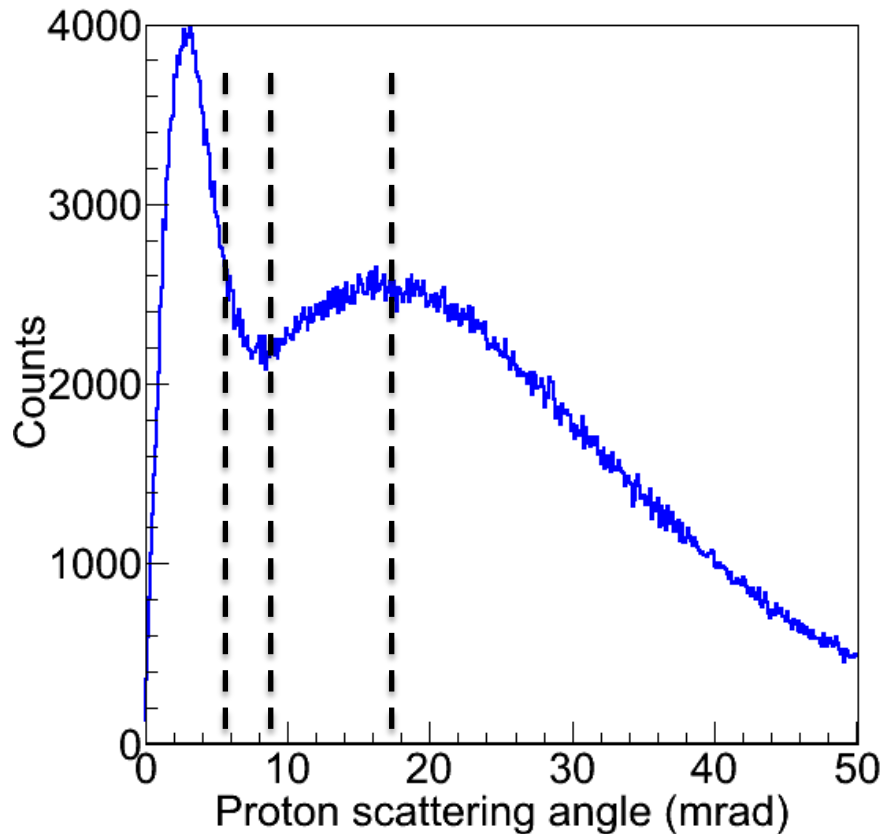
- ✧ Few materials on proton beam
- ✧ 11 various materials, including 5 tissue surrogates



Phantom material	Physical density (g/cm <sup>3</sup> )	Phantom material	Physical density (g/cm <sup>3</sup> )
Cortical bone*	1.820	Breast*	0.981
PMMA	1.180	Lung*	0.428
Liver*	1.095	Al	2.702
Adipose (fat)*	0.946	Ti	4.519
Air	0.0012	Cu	8.920
CT solid water	1.045	* Tissue-equivalent materials	

[https://www.sunnuclear.com/documents/datasheets/gammex/ct\\_electron\\_density\\_phantom.pdf](https://www.sunnuclear.com/documents/datasheets/gammex/ct_electron_density_phantom.pdf)

# Proton scattering angle, $\theta$

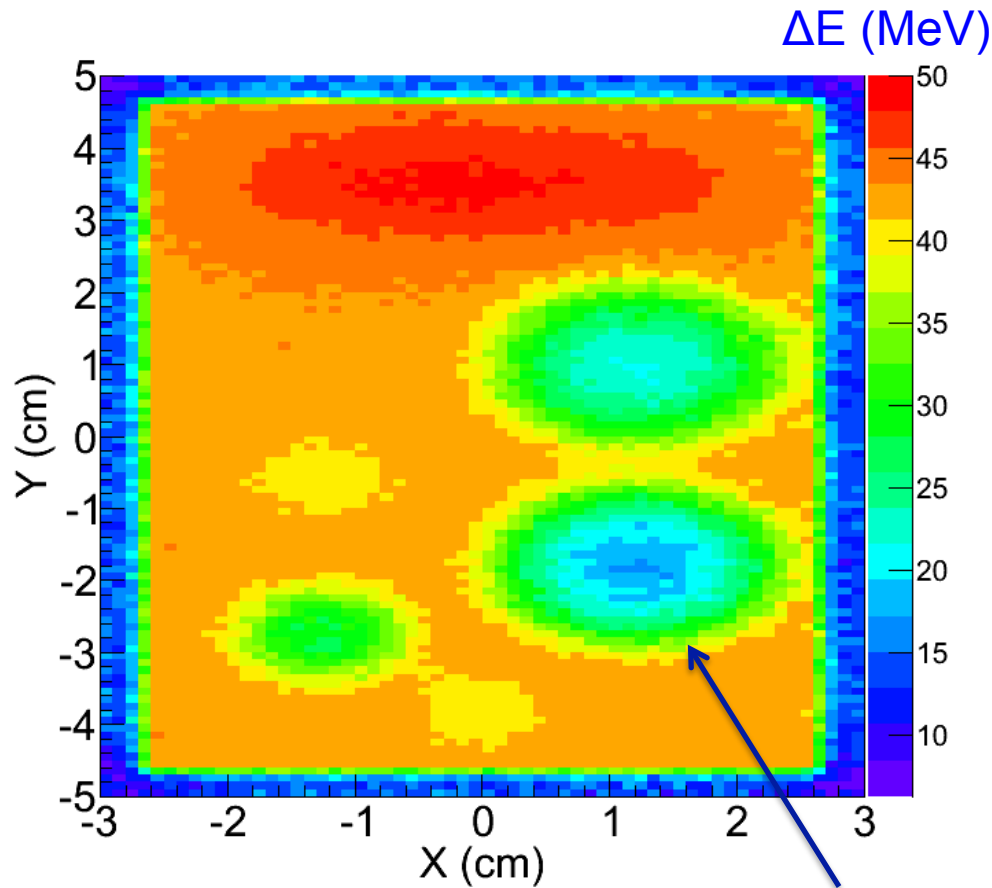


$$\theta(\text{rad}) = \cos^{-1} \left( \frac{\vec{p}_0 \cdot \vec{p}_3}{|\vec{p}_0| |\vec{p}_3|} \right)$$

$\vec{p}_0, \vec{p}_3$  – proton momenta  
in the source and energy  
detector, respectively

# Energy loss radiographs: $\Delta E = E_{\text{beam}} - E_{\text{residual}}$

- ✧ Protons that passed through all 3 detectors are considered



A.K. Biegun et al, JINST 11 (2016) C12015

Image blurred

Geant4 simulations

# Energy loss radiographs: $\Delta E = E_{\text{beam}} - E_{\text{residual}}$

✧ Protons that passed through all 3 detectors are considered

✧ Protons with maximum scattering angle  $\theta < 5.2$  mrad

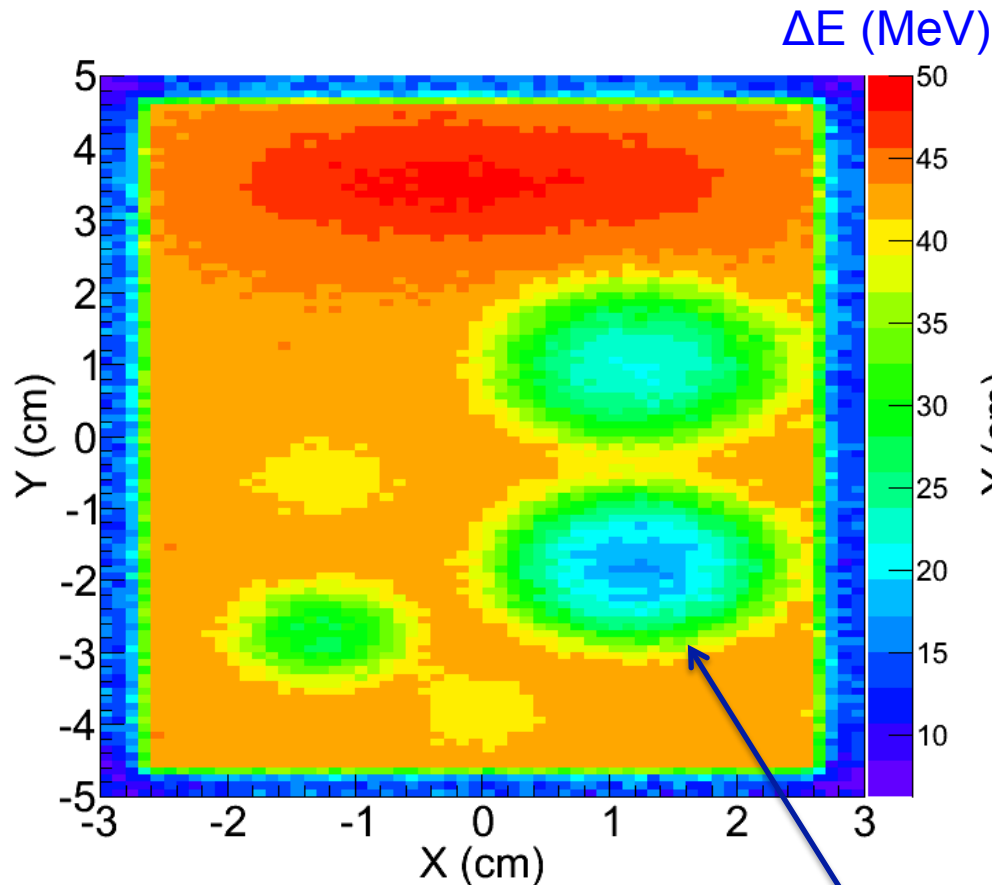
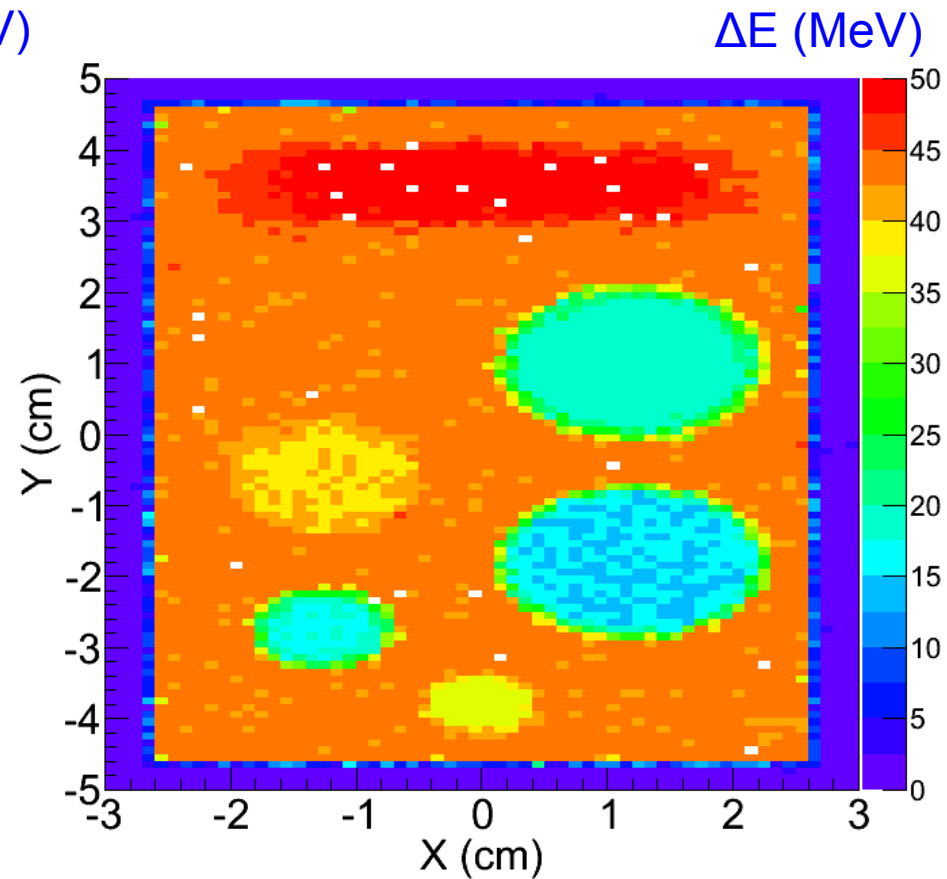


Image blurred

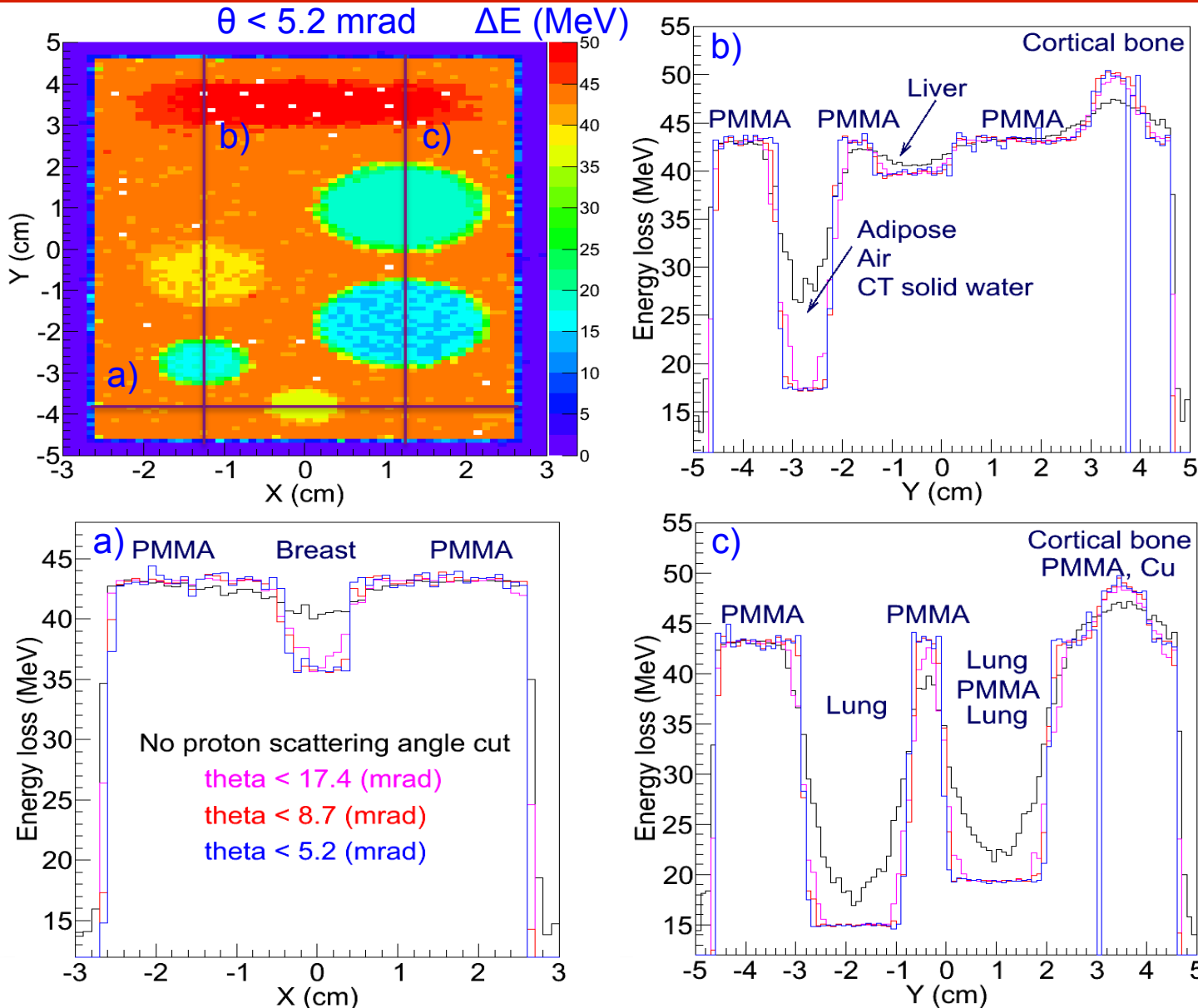


Geant4 simulations



# Energy loss radiographs: Projections

A.K. Biegun et al,  
 JINST 11 (2016) C12015

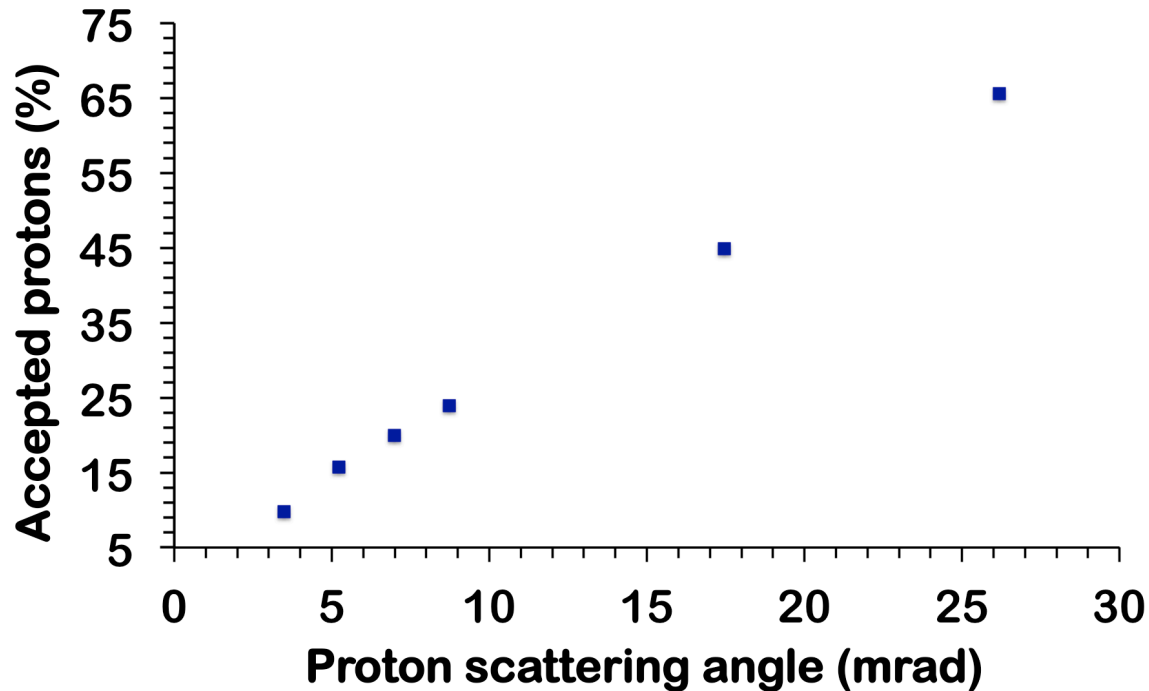


Sharper edges  
 between  
 materials for  
 smaller scattering  
 angles of protons

Bin size: 1 mm

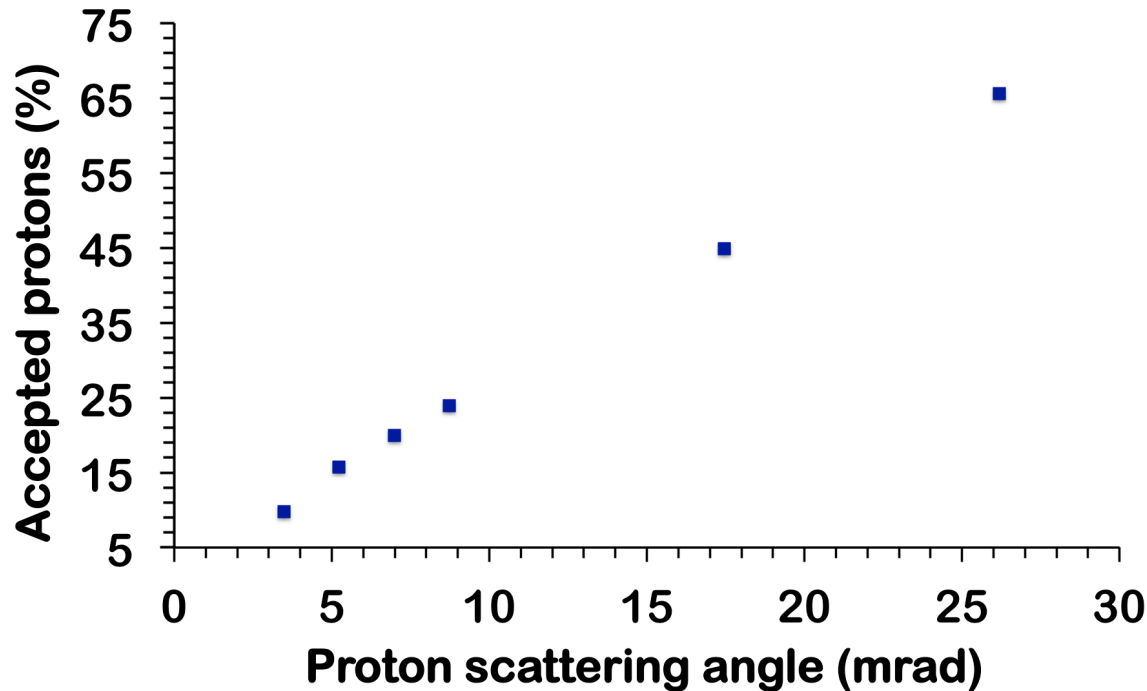
Geant4 simulations

# Statistics @ $E_p = 150$ MeV



$\theta$ (mrad)	Accepted protons (%)
26.2	65.6
17.4	44.9
8.7	23.9
6.7	20.0
5.2	15.7
3.5	9.8

# Statistics @ $E_p = 150$ MeV



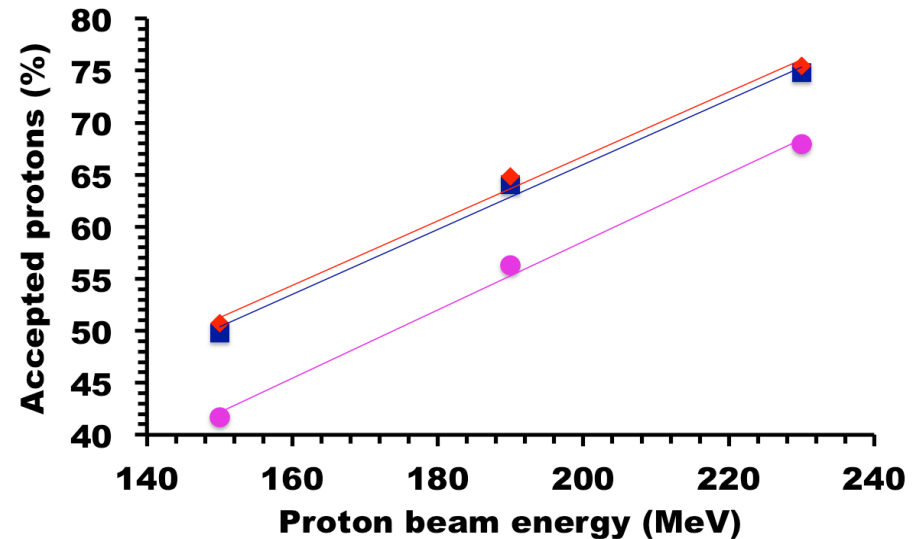
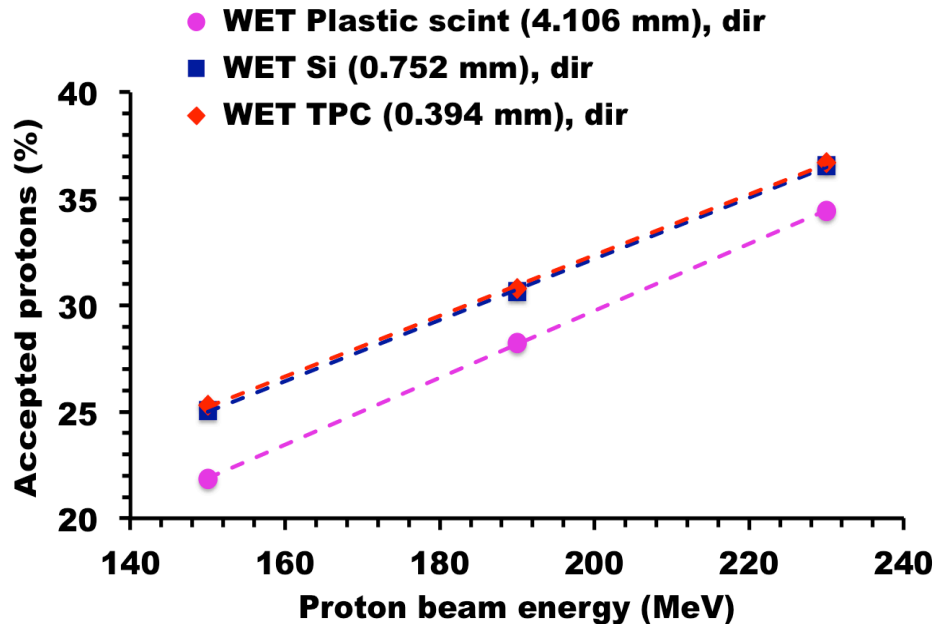
$\theta$ (mrad)	Accepted protons (%)
26.2	65.6
17.4	44.9
8.7	23.9
6.7	20.0
5.2	15.7
3.5	9.8

Significant number of protons (>70%) simulated at  $E_p=150$  MeV is eliminated at  $\theta < 8.7$  mrad

# Statistics @ $E_p = 150, 190$ and $230$ MeV

$$\diamond \theta_{12}^{\vec{p}} < 8.7 \text{ mrad}$$

$$\diamond \theta_{12}^{\text{pos}} < 8.7 \text{ mrad}$$



# Proton radiography @KVI-CART: Exp setup'15

Collaboration with J. Visser, M. van Beuzekom, E.N. Koffeman

## ✧ Tracking detectors:

- Timepix3-based TPC
- Count rate ~20 kHz

## ✧ Energy: BaF<sub>2</sub> scintillator

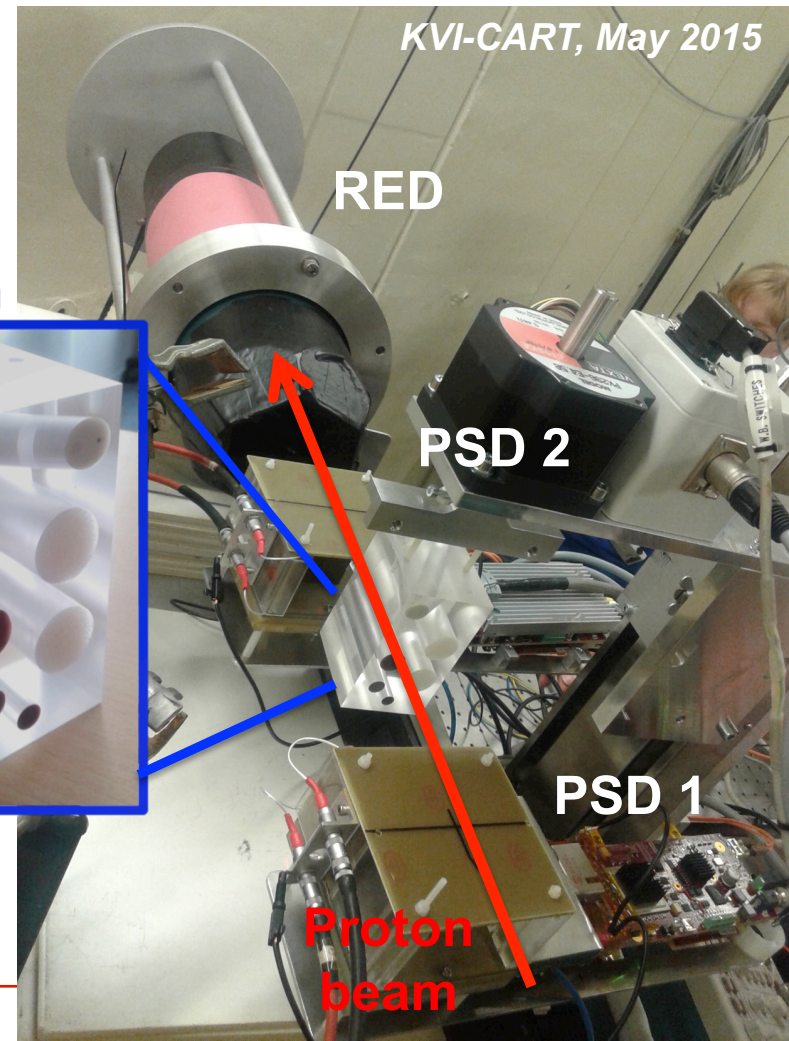
## ✧ Proton beam energy:

- $E_p = 150$  MeV

AGOR @KVI-CART  
Groningen (NL)

Count rate not yet high enough  
as required in clinics

Phantom



KVI-CART, May 2015

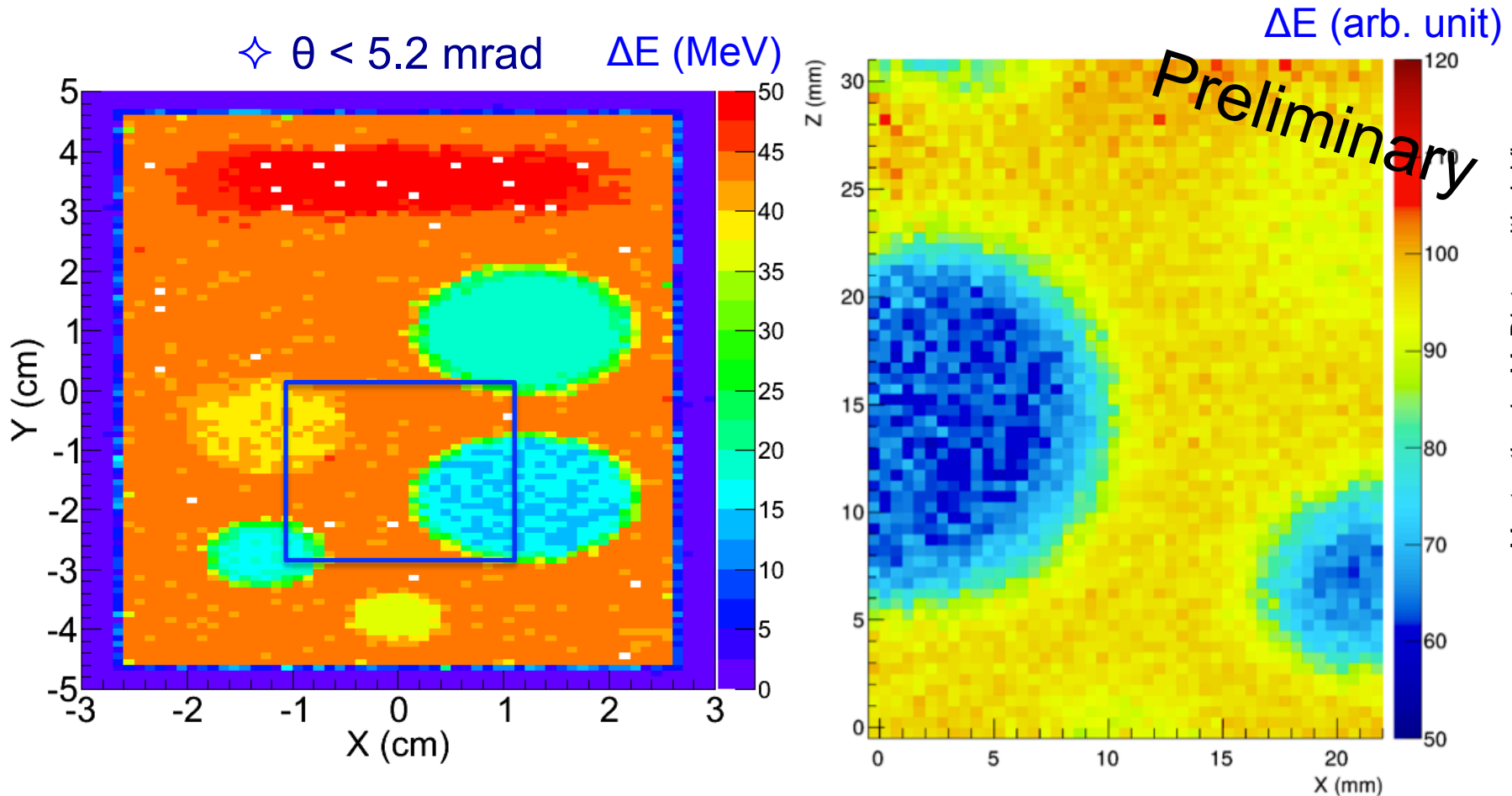
RED

PSD 2

PSD 1

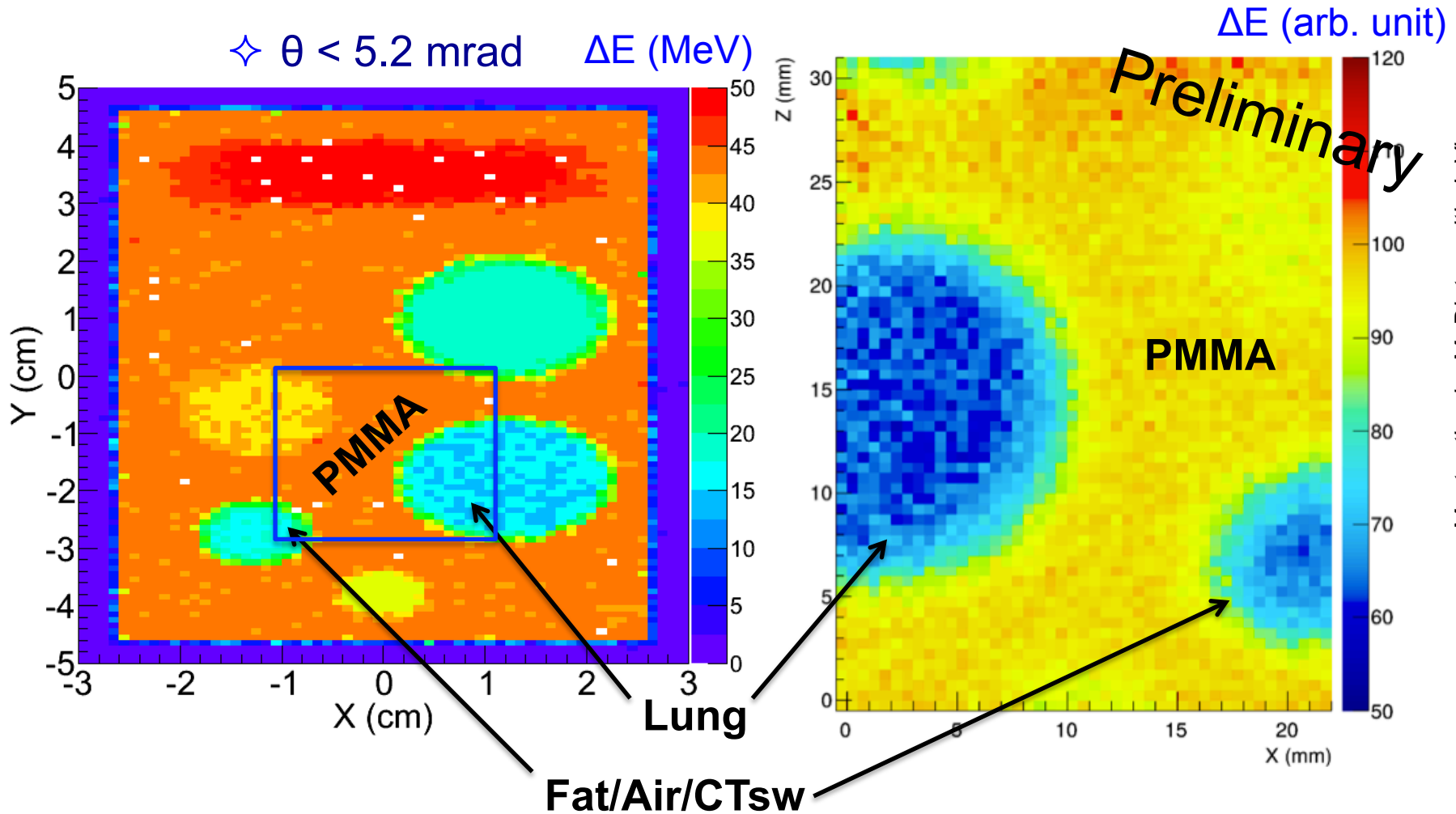
Proton  
beam

# Energy loss reconstruction: Sims vs. Exp'2015



◇ Phantom only partially covered by Timepix3-based TPCs ( $3.0 \times 3.0$  cm<sup>2</sup>)

# Energy loss reconstruction: Sims vs. Exp'2015

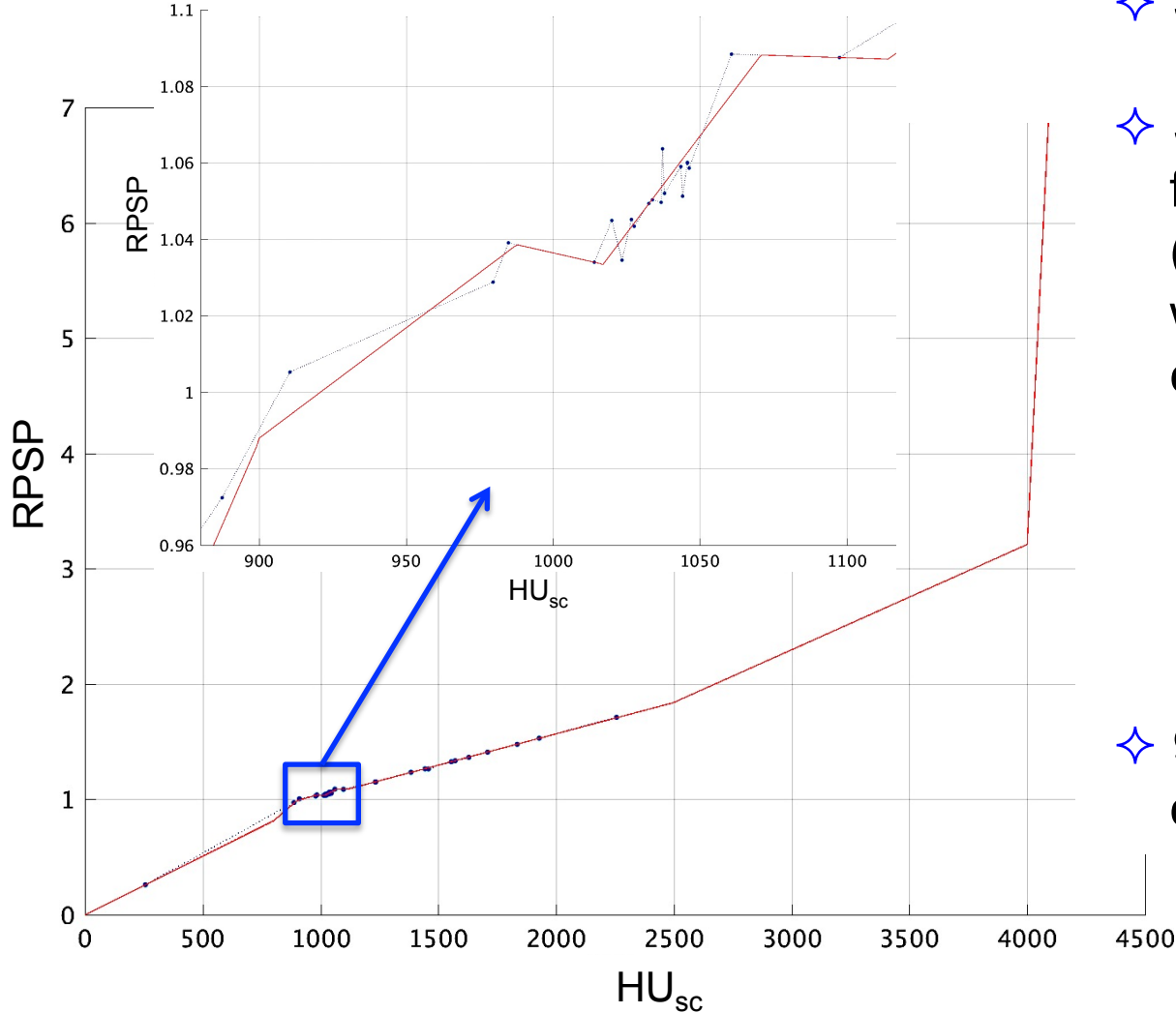


Simulations and experimental results comparable!



# Clinical calibration curve (120 kVp)

Master thesis: K. Ortega Marin with A.K. Biegun  
(KVI-CART/RuG July 2016)



- ✧ Specific for the scanner
- ✧ Stoichiometric method for biological tissues (35 standard human tissues) was used to obtain clinical calibration curve

*W. Snyder et al, Report of the Task Group on Reference Man, ICRP publication (1975)*

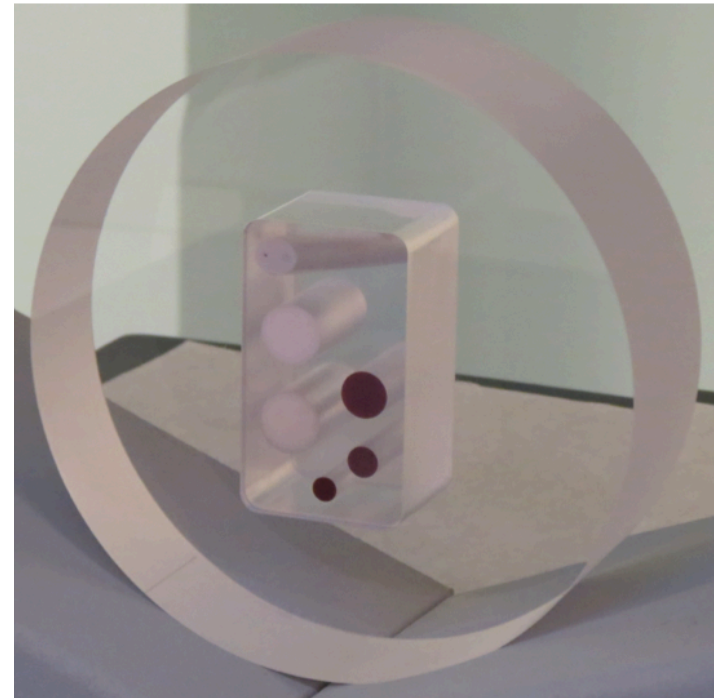
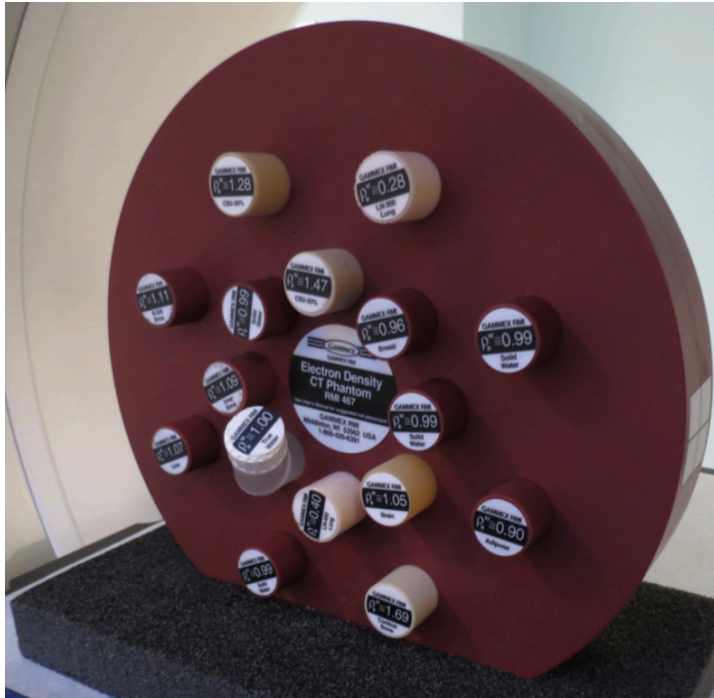
*U. Schneider, E. Pedroni, A. Lomax, PMB 41 (1996) 111*

- ✧ 9 linear segments in the calibration curve

$$HU_{sc} = 1000 * \mu / \mu_{water}$$
$$HU_{sc} = HU + 1000$$

# Gammex and Complex phantoms in CT scanner

- ✦ *Siemens Somatom Definition AS* (Radiotherapy department, UMCG)



December 2015. Acknowledgment to  
Arjen van der Schaaf, UMCG

- ✦ X-ray CT tube voltage:

- Gammex (*calibration*) phantom: **120 kVp**
- Complex (*patient*) phantom: 70, 80, 100, **120** and 140 **kVp**

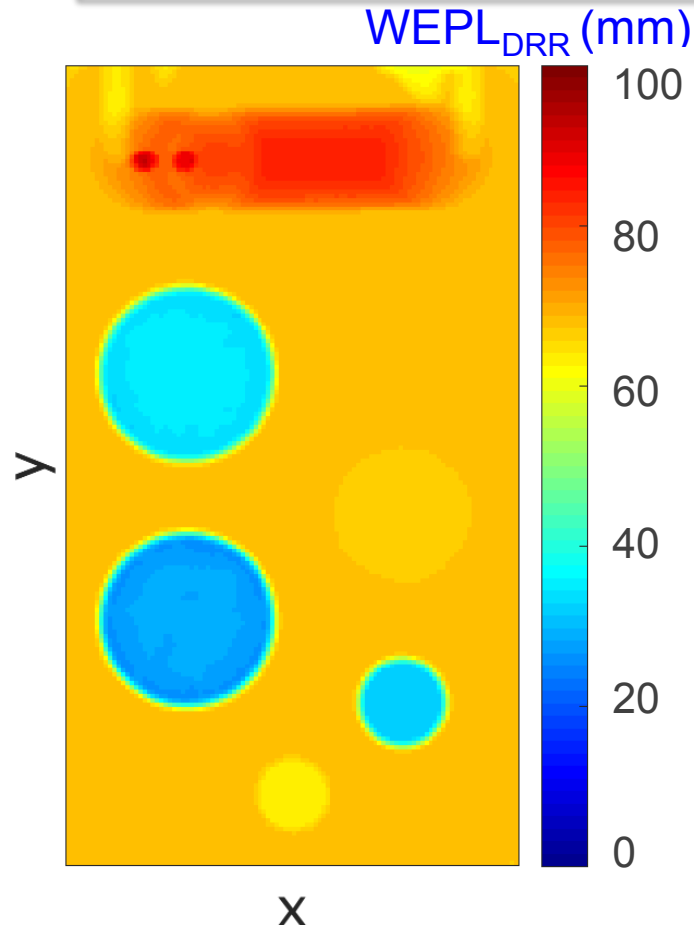
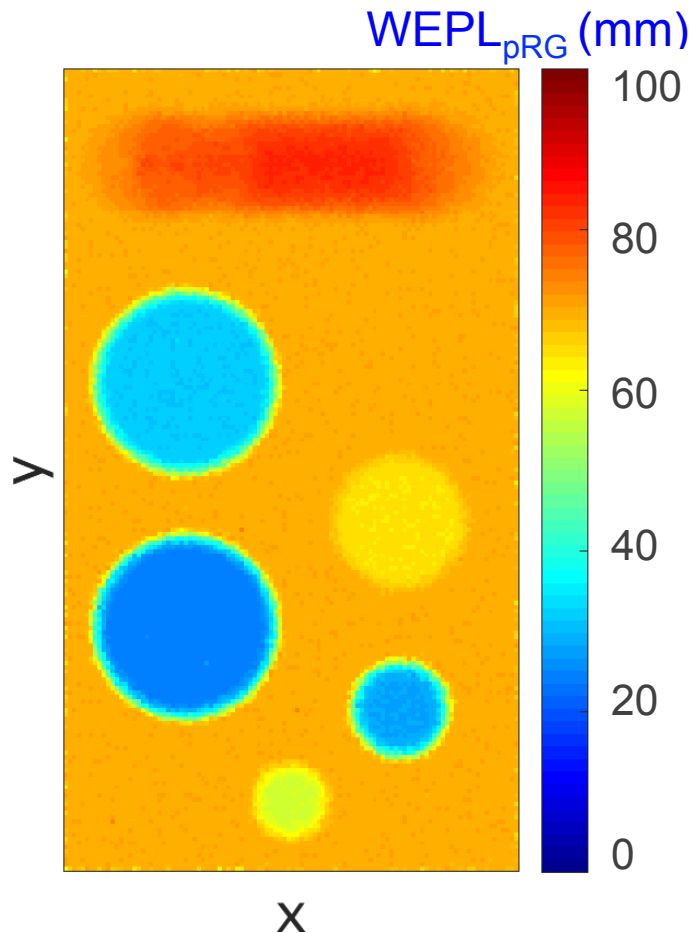
- ✦ CT scan of Gammex phantom to create a clinical calibration curve with tissue materials

# Water Equivalent Path Length (WEPL)

- ✧ Proton radiography:  
protons scattered < 5.2 mrad

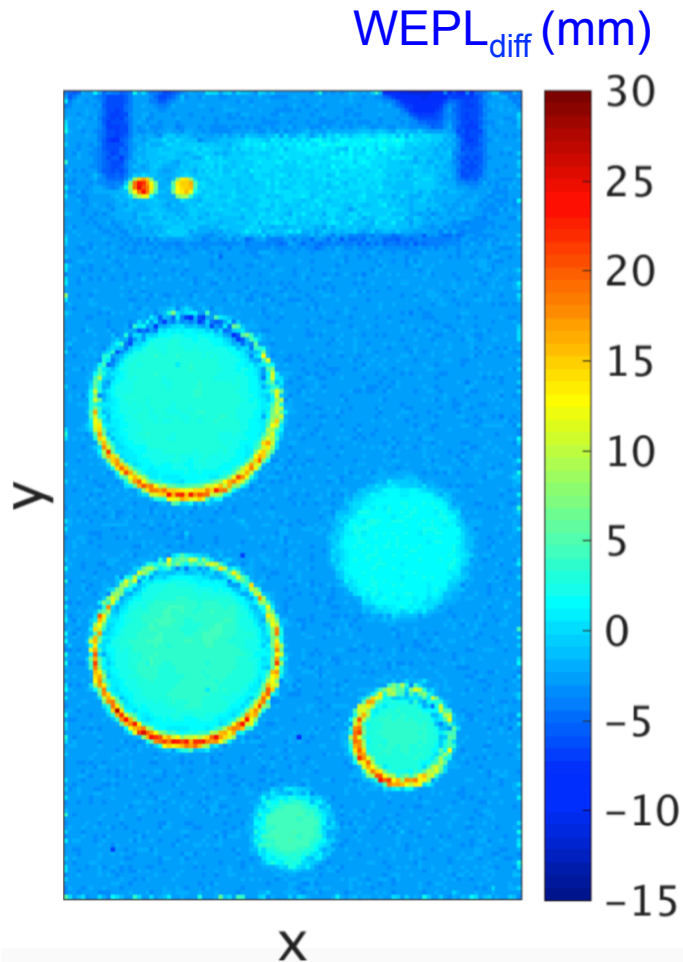
- ✧ X-ray CT @120 kVp

$$WEPL_{DRR(x,y)} = \sum_z \rho_s(HU_{SC}(x,y,z))\Delta z$$



# Difference between $WEPL_{DRR}$ and $WEPL_{pRG}$

Master thesis: K. Ortega Marin with A.K. Biegun  
(KVI-CART/RuG July 2016)



✧ Large overestimation in  $WEPL$   
at high density materials (Cu, Ti)

✧  $WEPL_{DRR} > WEPL_{pRG}$  in all inserts

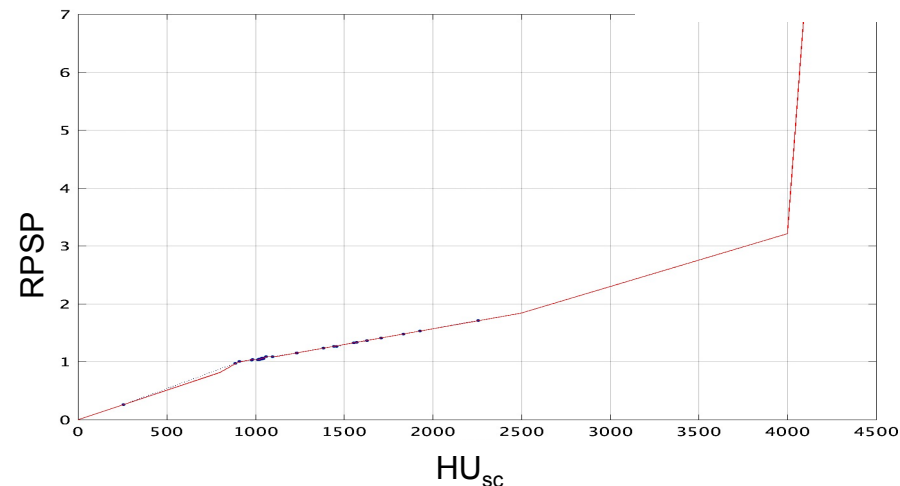
✧  $WEPL_{DRR} < WEPL_{pRG}$  in surrounding  
PMMA

→ PMMA not included  
in the clinical calibration curve

$$\text{RMSE} = \sqrt{\frac{\sum_{x,y} (\text{WEPL}_{\text{DRR}}(x,y) - \text{WEPL}_{\text{pRG}}(x,y))^2}{N}}$$

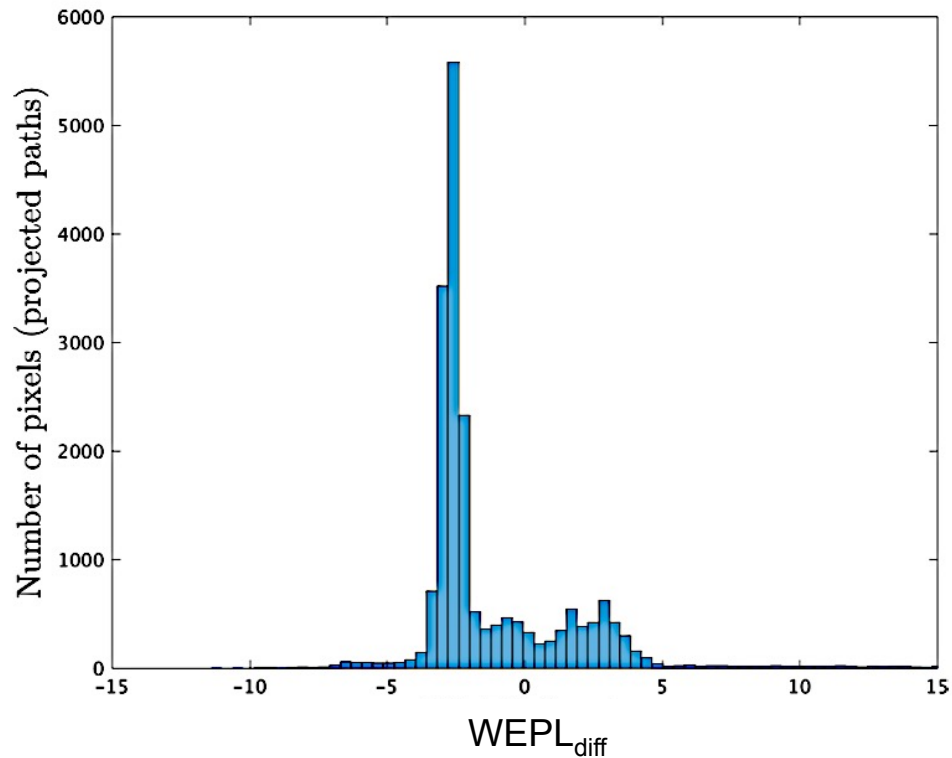
$$\chi^2 = \sum_{x,y} \frac{(\text{WEPL}_{\text{DRR}}(x,y) - \text{WEPL}_{\text{pRG}}(x,y))^2}{\text{WEPL}_{\text{pRG}}(x,y)}$$

- ✧ Modifications of RPSP splitting point for 9 segments were done after either RMSE or  $\chi^2$  was minimized

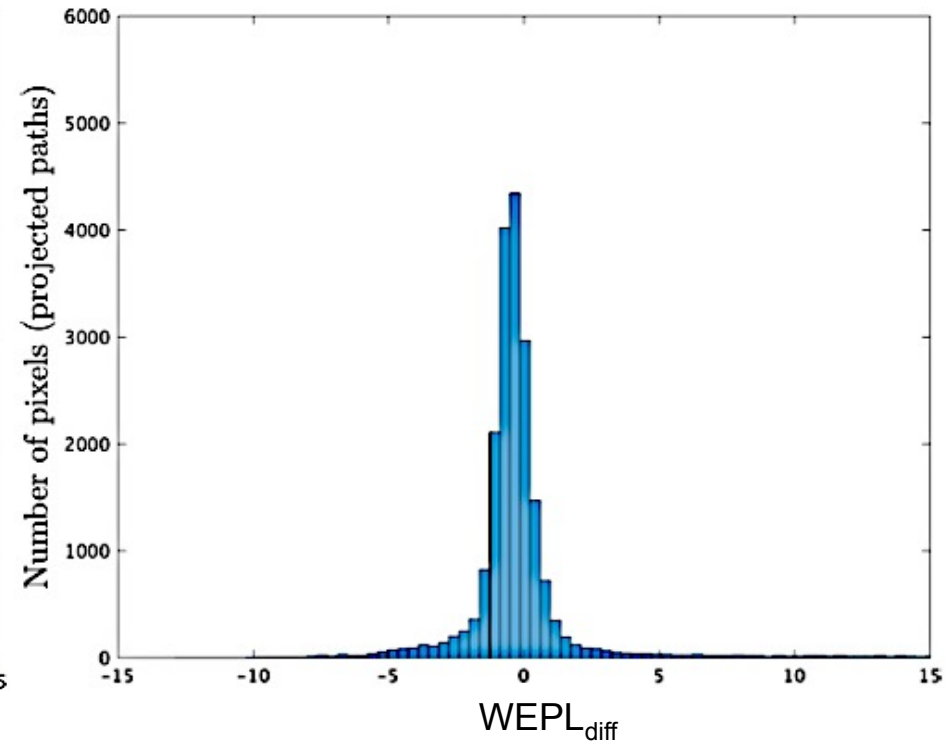


# Number of pixels with certain WEPL

✧ Difference **before** optimization



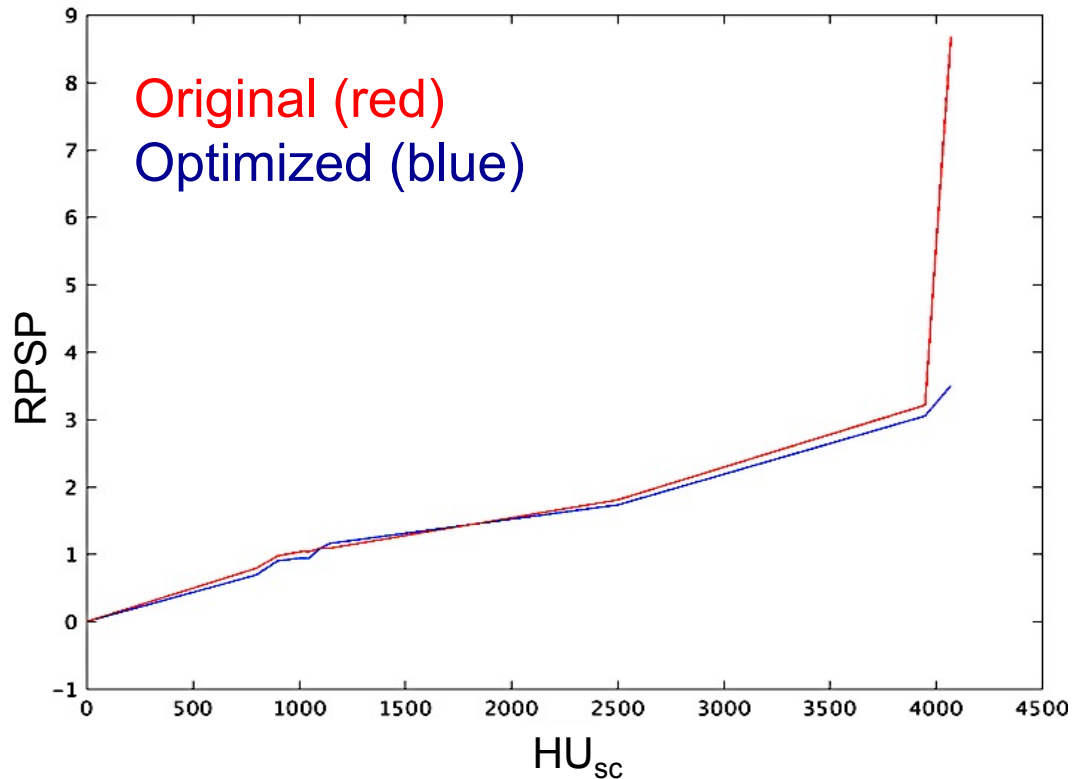
✧ Difference **after** optimization



✧ Large fraction of pixels have a difference in WEPL between -2.5 mm and -3.5 mm (PMMA)

# Original & optimized clinical calibration curves

Master thesis: K. Ortega Marin with A.K. Biegun  
(KVI-CART/RuG July 2016)



## Before optimization

Metric	With PMMA
RMSE	3.59 mm
$\chi^2$	5083.80

## After optimization

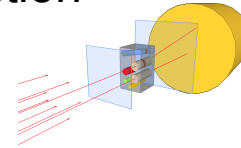
Metric	With PMMA
RMSE	2.36 mm (-34.33%)
$\chi^2$	2287.10 (-55.01%)



# Summary

pRG

- ✧ Delivers proton stopping powers directly
- ✧ MCS decreases image quality, but angular selection improves it
- ✧ Experiments and simulations with the Complex (patient) phantom have been done



- Experimental results of  $\Delta E$  are comparable with simulations
- $WEPL_{pRG}$

X-ray CT

- ✧ CT scans of Gammex (calibration) and Complex (patient) phantoms



+



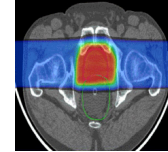
- $WEPL_{DRR}$

pRG + X-ray CT

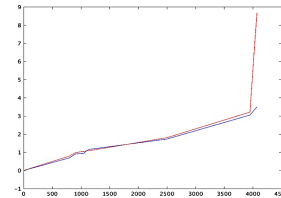
- ✧  $WEPL_{DRR} - WEPL_{pRG}$
- ✧ Optimization of the “patient-specific” calibration curve for Complex (patient) phantom

- $WEPL_{diff}$
- Optimized RPSP for treatment planning

- Compare proton treatment plan before / after optimization



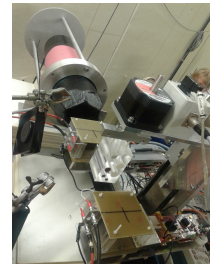
- Further optimization of the clinical calibration curve:  
 split of each segments into smaller segments  
 to account for larger heterogeneities in human tissue



- Include CT/DECT patient data in Geant4 MC pRG simulations



- Development of detectors (tracking and energy) for pRG  
 to achieve clinically relevant count rates ( $> \text{MHz}$ )

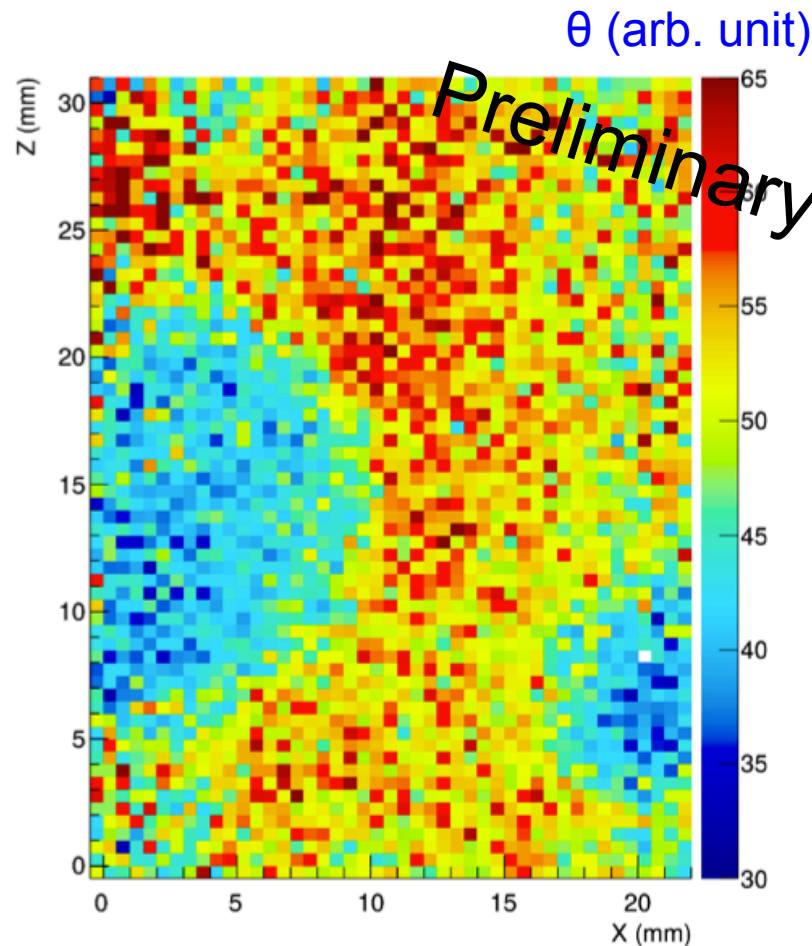


- Validate Geant4 MC simulations with the pRG experimental data

# Backup slides



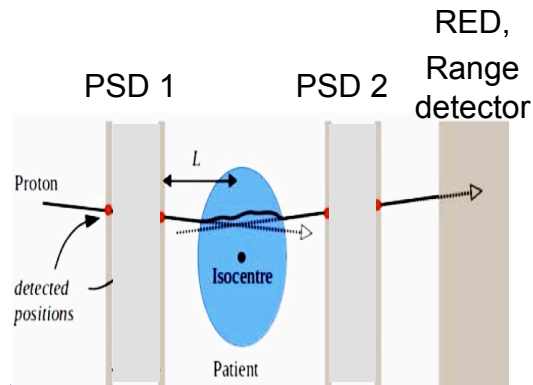
# Scattering angle reconstruction: Exp'2015



Master thesis: M. Dietze with J. Visser,  
M. van Beuzekom, E. Koffeman (Nikhef June 2016)

Scattering angle well reconstructed, but more statistics needed

# Current systems



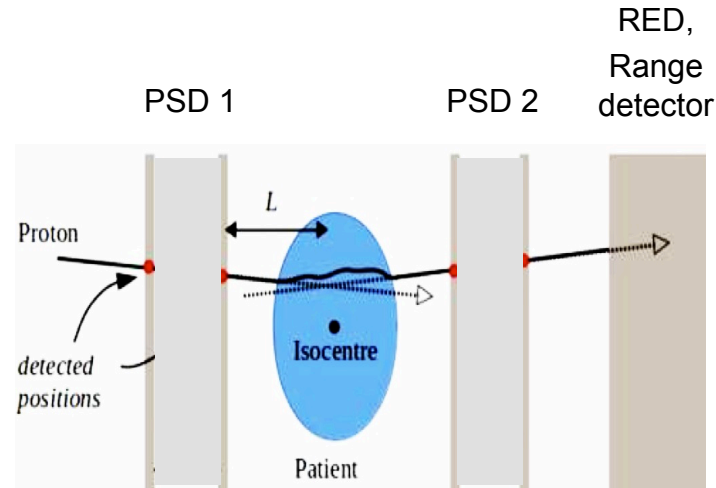
Group	Year	PSDs (# of units)	RED/Range Detector	Rate (Hz)	Imaging device
PSI	2005	x-y Sci-Fi (4)	Plastic scintillator telescope	1 M	pRad
LLU/UCSC/NIU	2013	x-y SiSDs (4)	CsI (TI)	15 k	pCT
LLU/UCSC/CSUSB	2014	x-y SiSDs (4)	Plastic scintillator hybrid telescope	2 M	pCT
AQUA	2013	x-y GEMs (2)	Plastic scintillator telescope	1 M	pRad
PRIMA I	2014	x-y SiSDs (4)	YAG:Ce calorimeter	10 k	pCT
PRIMA II	2014	x-y SiSDs (4)	YAG:Ce calorimeter	1 M	pCT
INFN	2014	x-y Sci-Fi (4)	x-y Sci-Fi	1 M	pCT
NIU/FNAL	2014	x-y Sci-Fi (4)	Plastic scintillator telescope	2 M	pCT
Niigata University	2014	x-y SiSDs (4)	NaI (TI) calorimeter	5 k	pCT
PRaVDA	2015	X-u-v SiSDs	CMOS APS telescope	1 M	pCT

✧ Trend towards Si tracking detectors  
→ very fast

✧ Different approaches for energy/range detectors

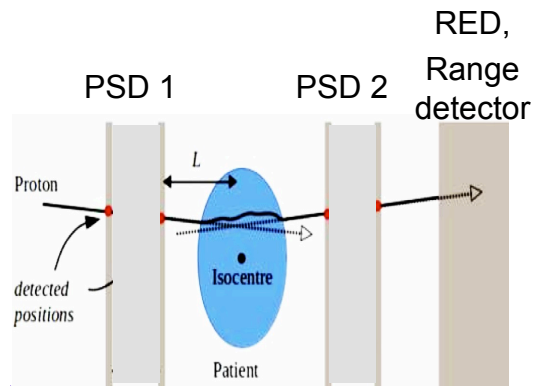
✧ Count rate close to what is required

# But...



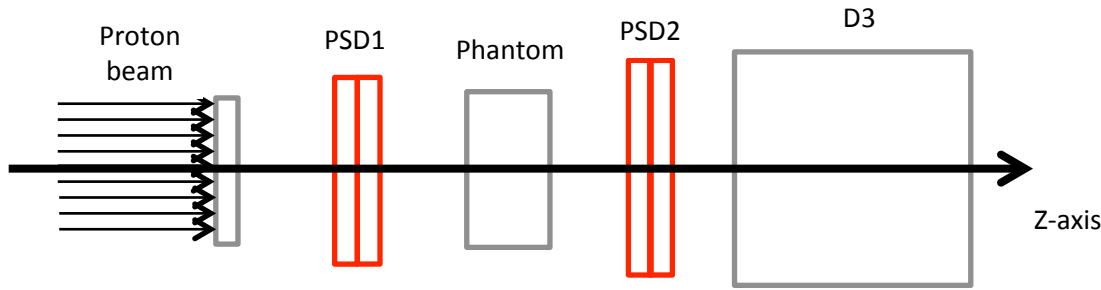
- ✧ Si ( $Z=14$ ,  $\rho=2.33 \text{ g/cm}^3$ )  
→ Multiple Coulomb Scattering already in the detector material
- ✧ Range detector does not give yet accurate enough residual energy important for proton stopping powers determination of an object

# Simulations for:

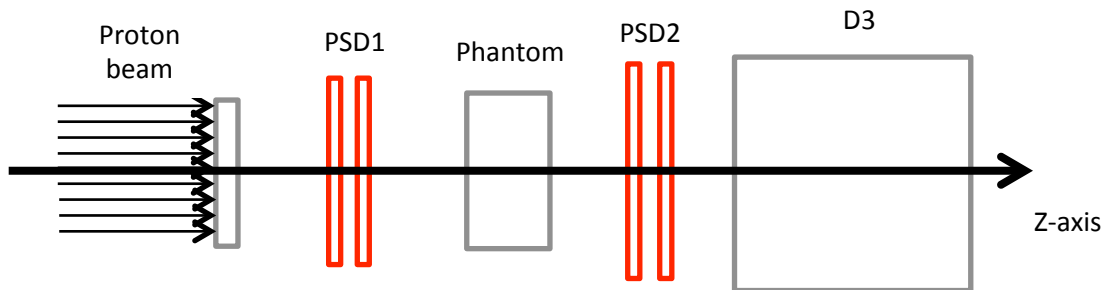


Group	Year	PSDs (# of units)	RED/Range Detector	Rate (Hz)	Imaging device
PSI	2005	x-y Sci-Fi (4)	Plastic scintillator telescope	1 M	pRad
LLU/UCSC/NIU	2013	x-y SiSDs (4)	CsI (TI)	15 k	pCT
LLU/UCSC/CSUSB	2014	x-y SiSDs (4)	Plastic scintillator hybrid telescope	2 M	pCT
AQUA	2013	x-y GEMs (2)	Plastic scintillator telescope	1 M	pRad
PRIMA I	2014	x-y SiSDs (4)	YAG:Ce calorimeter	10 k	pCT
PRIMA II	2014	x-y SiSDs (4)	YAG:Ce calorimeter	1 M	pCT
INFN	2014	x-y Sci-Fi (4)	x-y Sci-Fi	1 M	pCT
NIU/FNAL	2014	x-y Sci-Fi (4)	Plastic scintillator telescope	2 M	pCT
Niigata University	2014	x-y SiSDs (4)	NaI (TI) calorimeter	5 k	pCT
PRaVDA	2015	X-u-v SiSDs	CMOS APS telescope	1 M	pCT

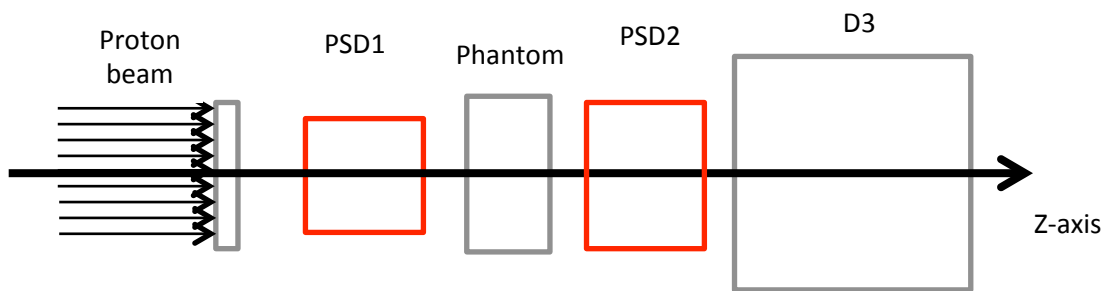
# Various PSDs in proton radiography setup



✧ Two plane  
 fiber scintillating hodoscope  
 (PSI)



✧ Two plane  
 silicon strip detectors  
 (PRIMA I)



✧ Time Projection Chamber  
 (Nikhef)

Geant4 simulations



# PSDs parameters

PSD detector type	Number of PSDs	Material	Material thickness (mm)	Material density (g/cm <sup>3</sup> )	WET (mm)
Ideal	1	Air	0.001	0.0012	-
Plastic scintillator Fiber [1]	2	Bicron BCF12	4.0	1.032	4.106
Silicon strip detector [2]	2	Silicon	0.4	2.33	0.752
Gaseous TPC [3]	1	Isobutene C <sub>4</sub> H <sub>10</sub>	30	0.0025	0.394

[1] U. Schneider et al., *Med Phys* 31:5 (2014) 1046-1051

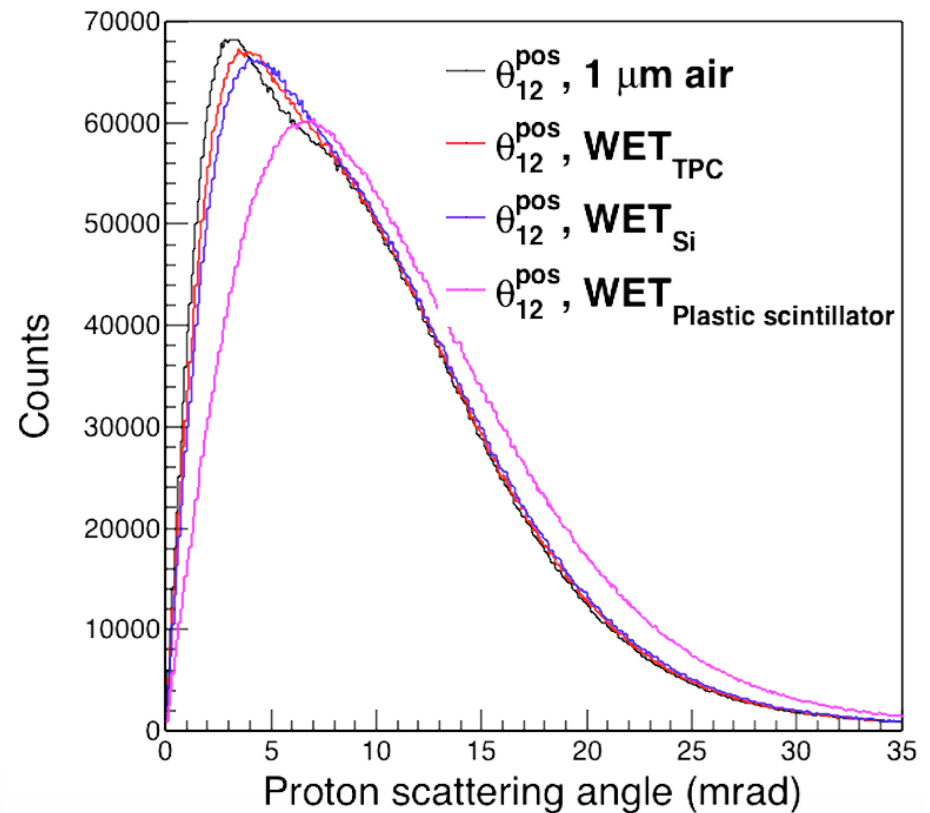
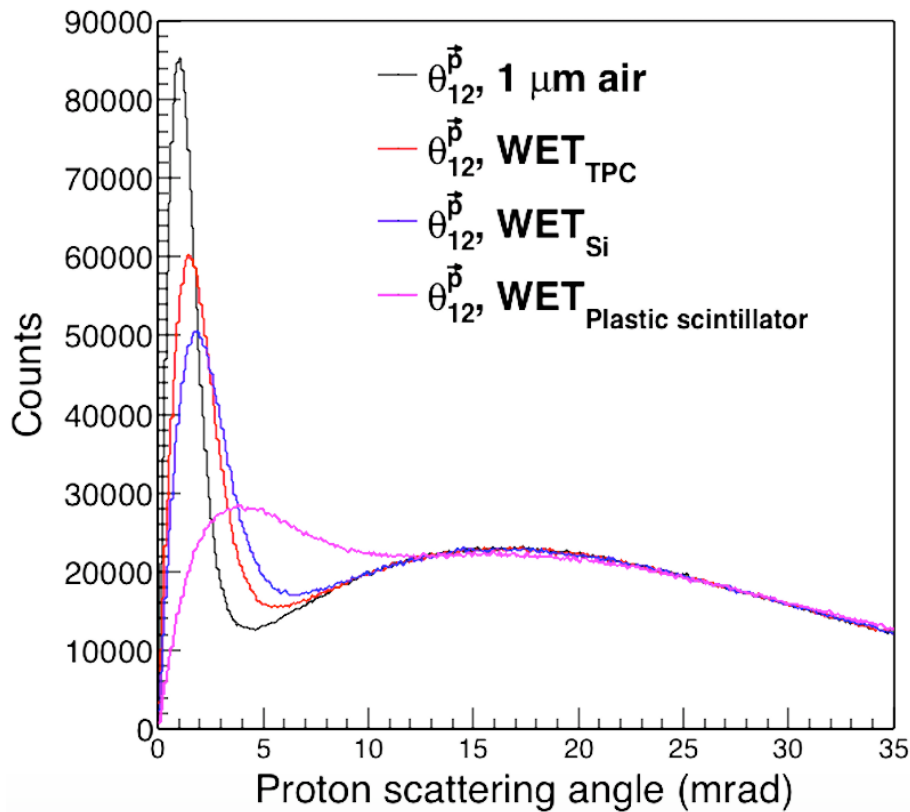
[2] M. Scaringella et al., *JINST* 9 (2014) C12009

[3] A.K. Biegun et al., *JINST* 11 (2016) C12015

# Statistics @ $E_p = 150, 190$ and $230$ MeV

$$\phi_{12}^p(\text{rad}) = \cos^{-1} \frac{\vec{p}_1 \cdot \vec{p}_2}{|\vec{p}_1| |\vec{p}_2|}$$

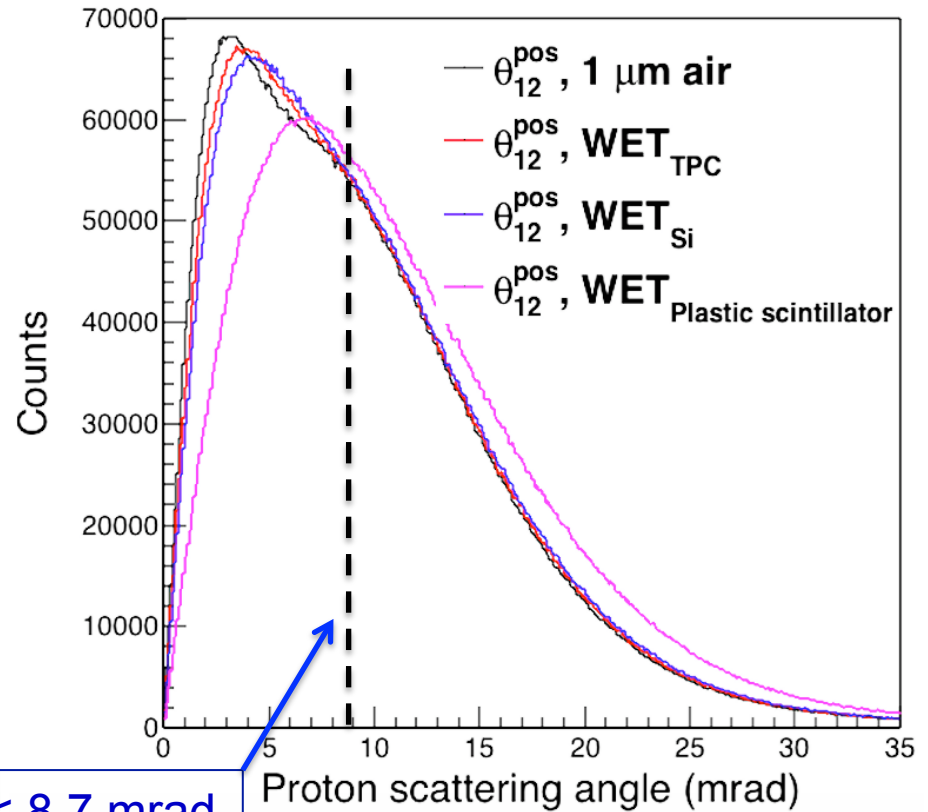
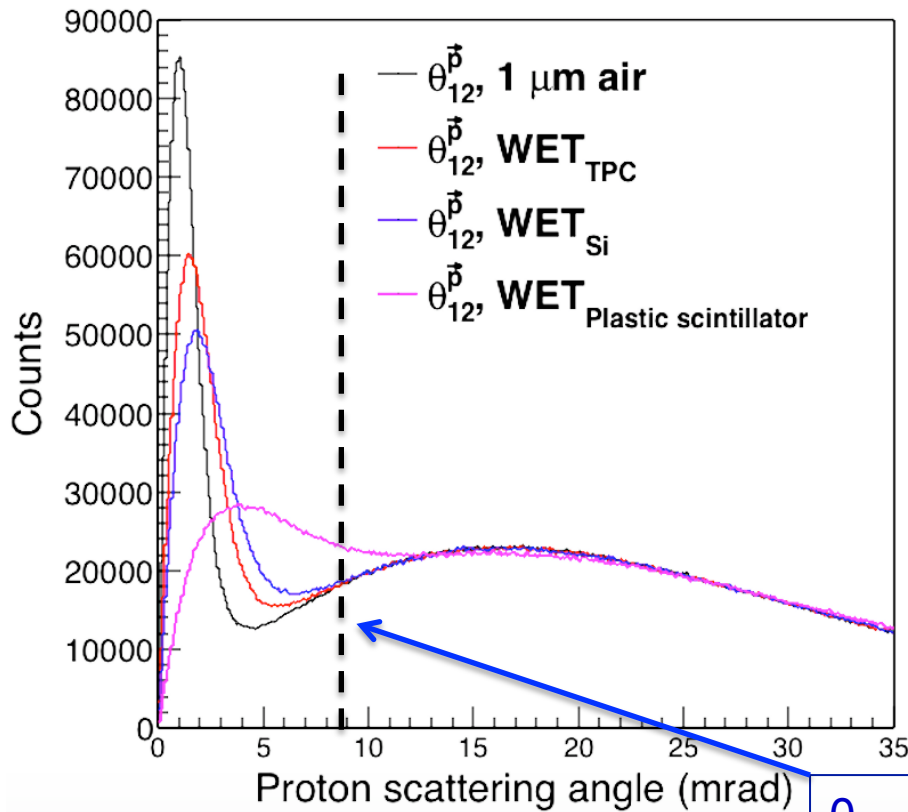
$$\phi_{12}^{pos}(\text{rad}) = \tan^{-1} \frac{\sqrt{(x_2 - x_1)^2 + (y_2 - y_1)^2}}{(z_2 - z_1)}$$



# Statistics @ $E_p = 150, 190$ and $230$ MeV

$$\phi_{12}^p(\text{rad}) = \cos^{-1} \frac{\vec{p}_1 \cdot \vec{p}_2}{|\vec{p}_1| |\vec{p}_2|}$$

$$\phi_{12}^{\text{pos}}(\text{rad}) = \tan^{-1} \frac{\sqrt{(x_2 - x_1)^2 + (y_2 - y_1)^2}}{(z_2 - z_1)}$$



$\theta_{12} < 8.7$  mrad

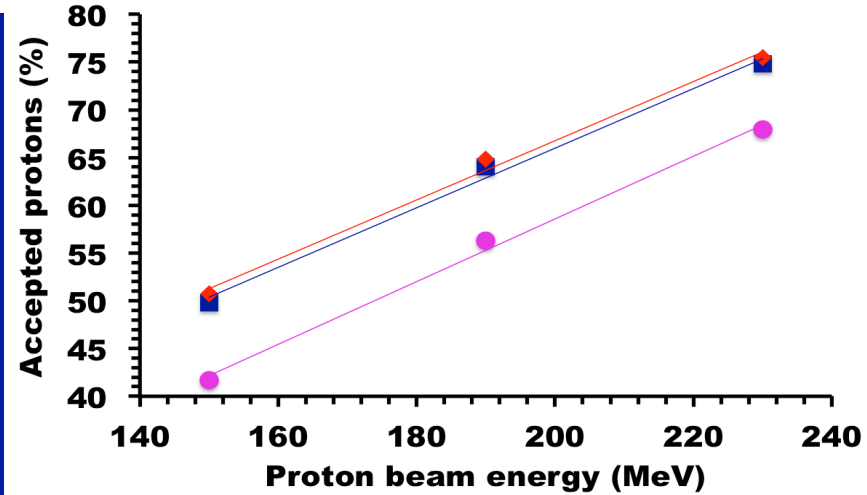
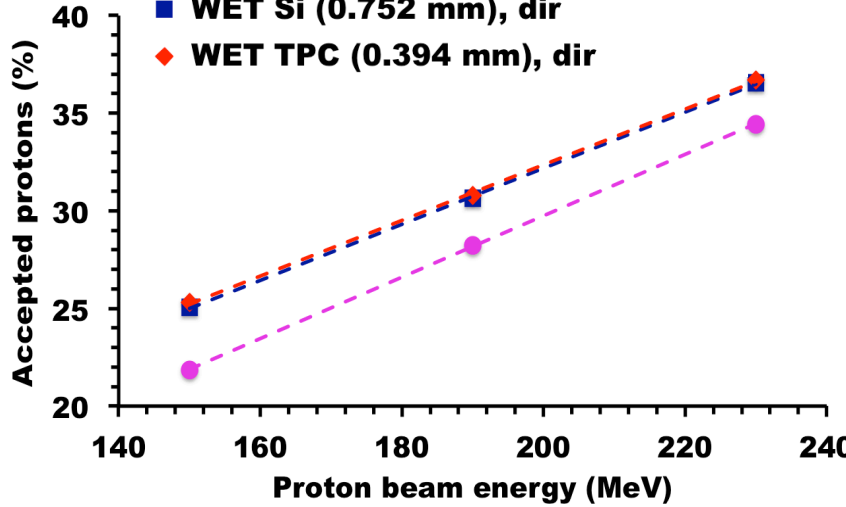
Geant4 simulations

# Statistics @ $E_p = 150, 190$ and $230$ MeV

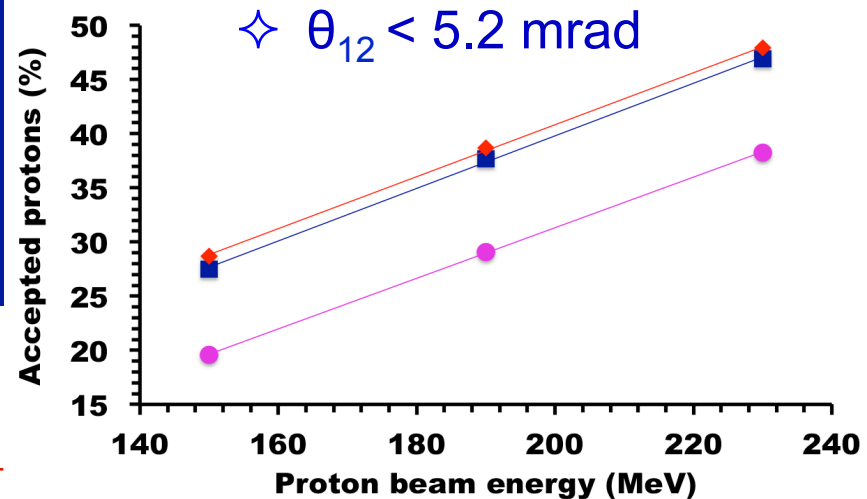
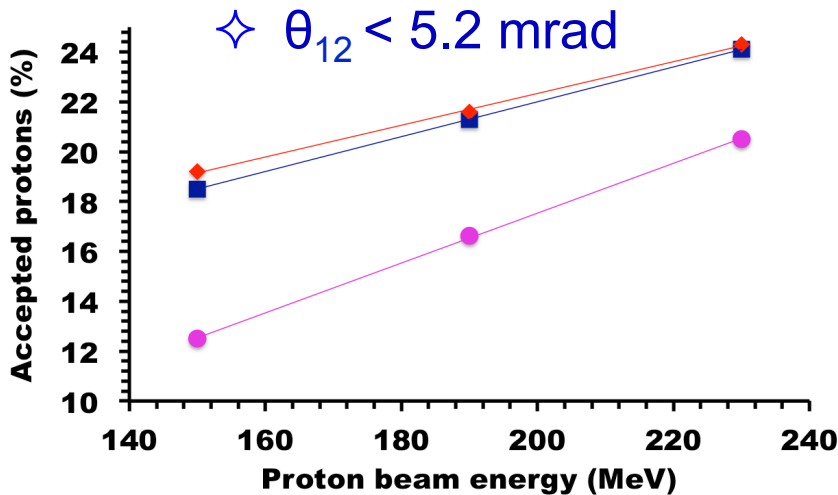
✧  $\theta_{12} < 8.7$  mrad

✧  $\theta_{12} < 8.7$  mrad

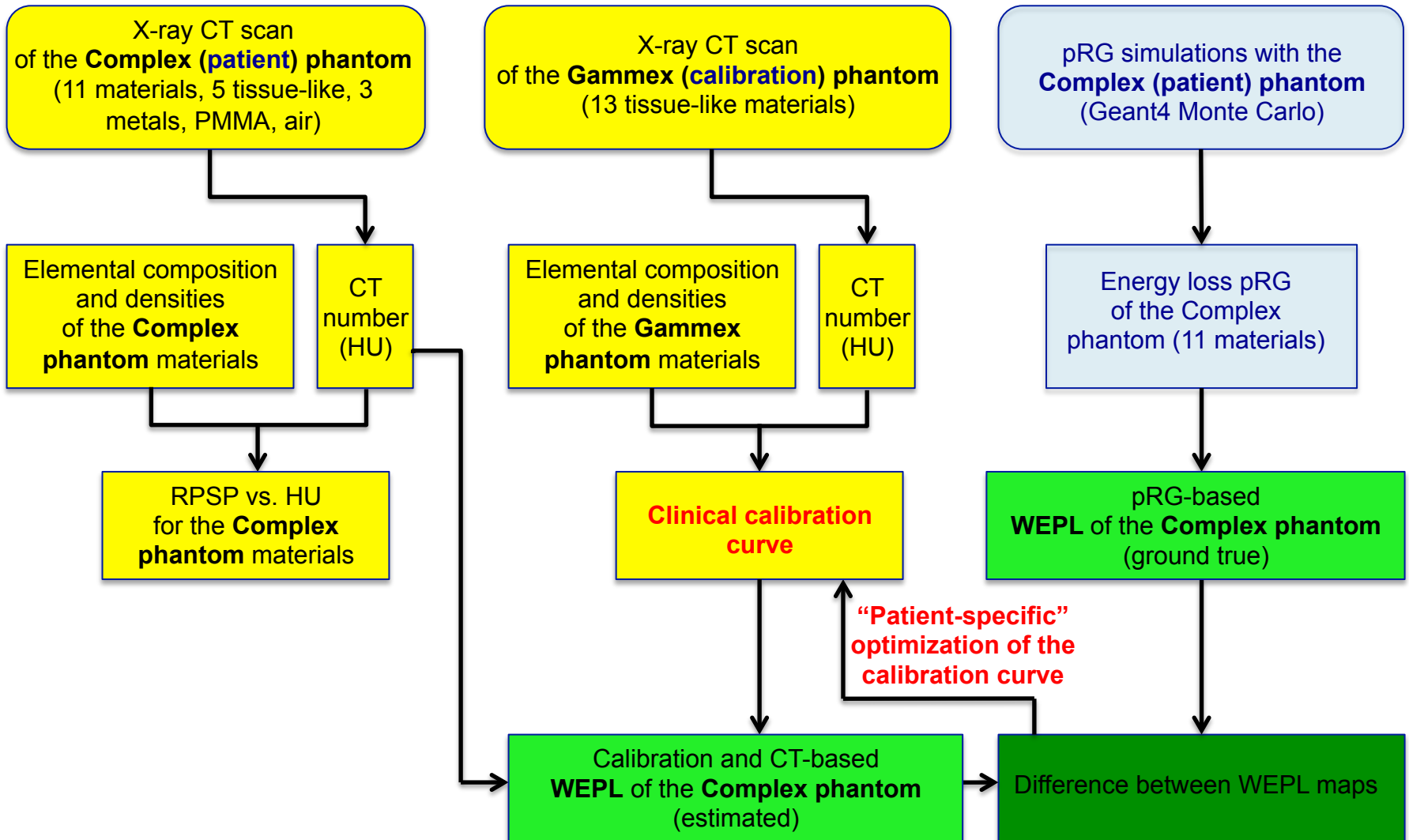
- WET Plastic scint (4.106 mm), dir
- WET Si (0.752 mm), dir
- ◆ WET TPC (0.394 mm), dir



position ( $x, y, z$ )



# Work flow diagram



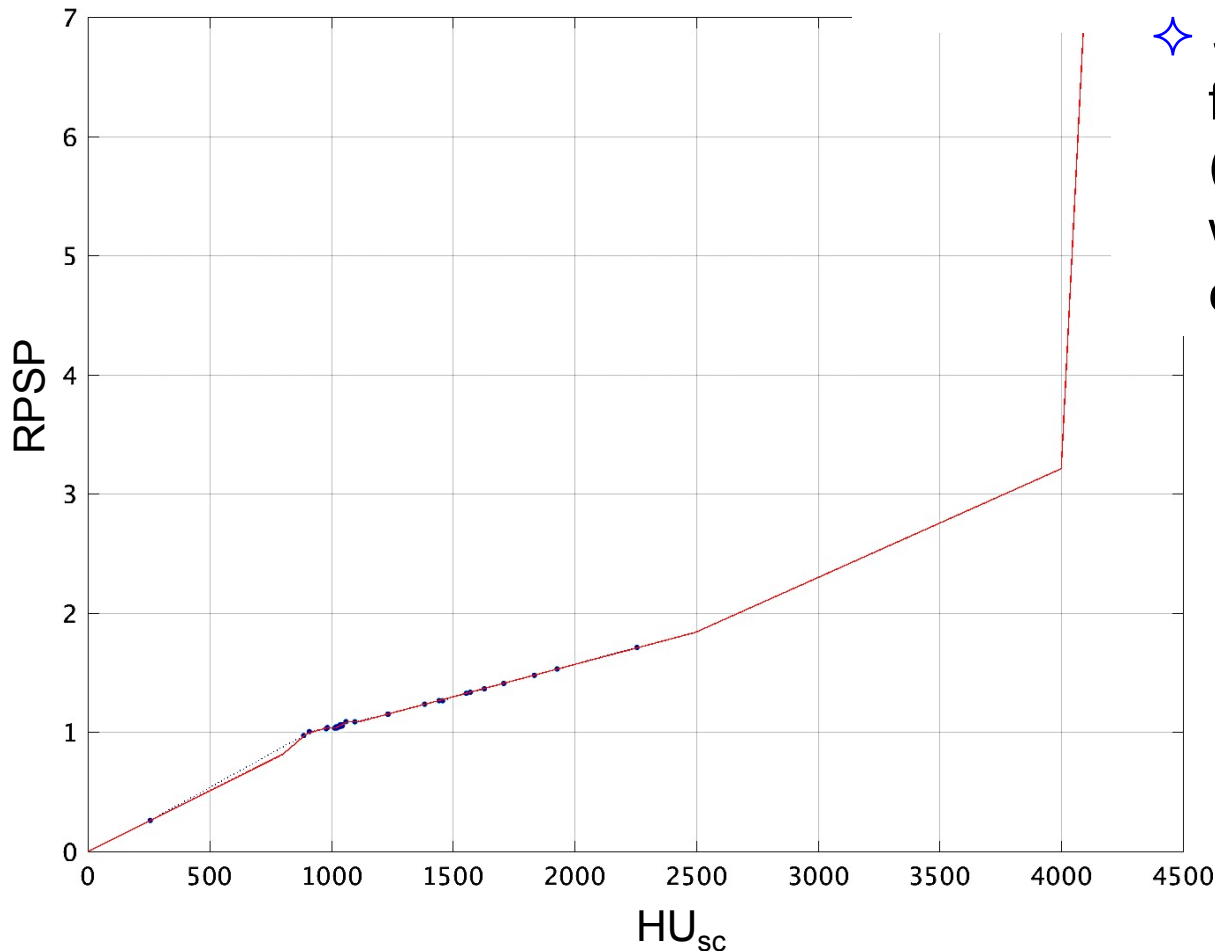
K. Ortega Marin, MSc thesis, KVI-CART/RuG (2016)

# Clinical calibration curve (120 kVp)

Master thesis: K. Ortega Marin with A.K. Biegun  
(KVI-CART/RuG July 2016)

✧ Specific for the scanner

✧ Stoichiometric method  
for biological tissues  
(35 standard human tissues)  
was used to obtain  
clinical calibration curve



*W. Snyder et al, Report of the Task Group on  
Reference Man, ICRP publication (1975)*

*U. Schneider, E. Pedroni, A. Lomax,  
PMB 41 (1996) 111*

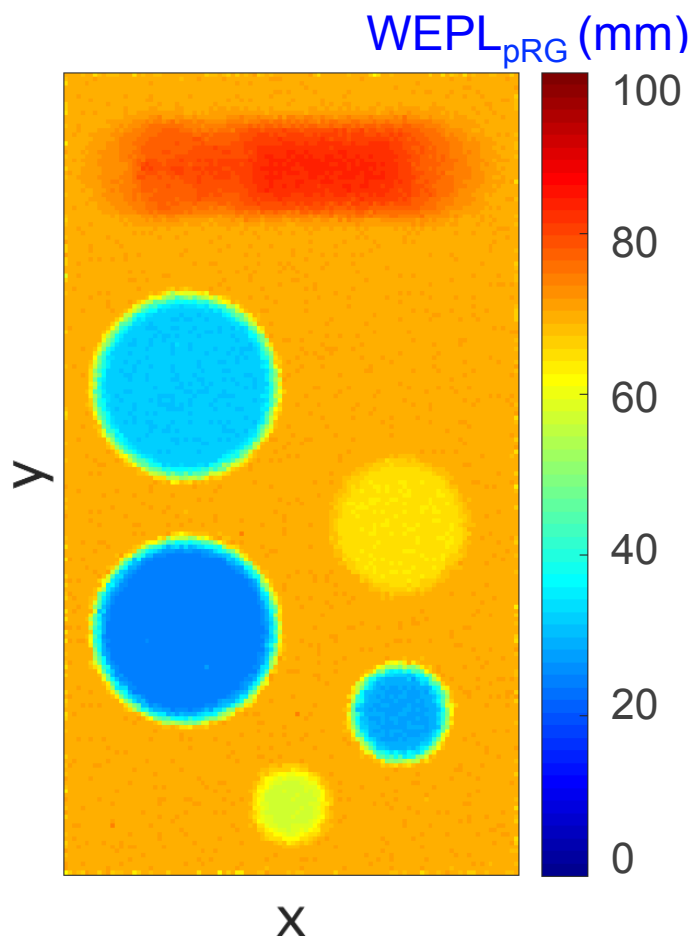
$$HU_{sc} = 1000 * \mu / \mu_{water}$$
$$HU_{sc} = HU + 1000$$

# Water Equivalent Path Length (WEPL)

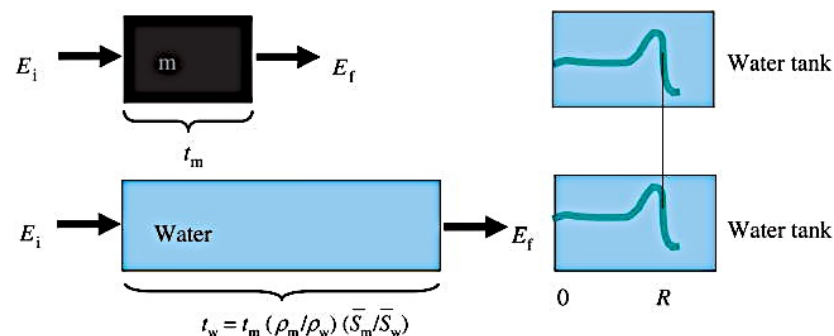
- Proton radiography:  
protons scattered  $< 5.2$  mrad

Voxel size:  $1 \times 1 \times 6$  mm<sup>3</sup>

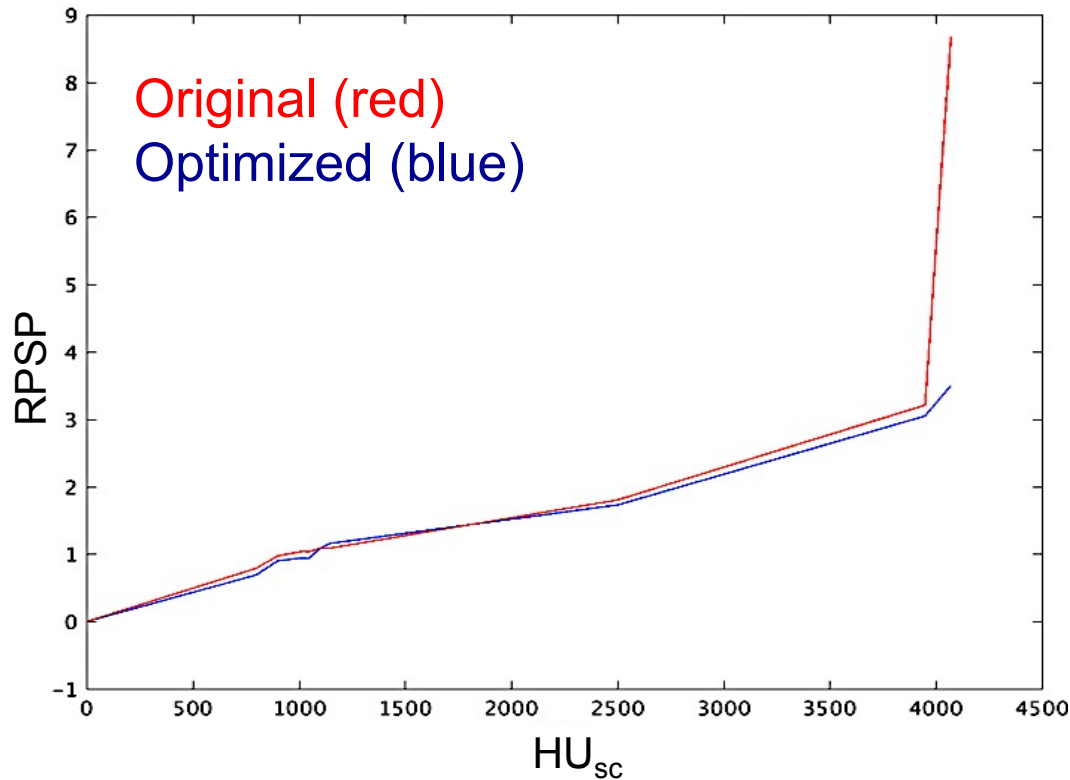
$$WEPL_{pRG} = t_m \times \rho_s = t_m \frac{\rho_m}{\rho_w} \frac{\bar{S}_m}{\bar{S}_w}$$



**WEPL of material** – thickness  $t_w$  of water, in which a proton with an energy  $E_i$  will stop at the same range as after passing a thickness  $t_m$  of the material



# Original & optimized clinical calibration curves



## Before optimization

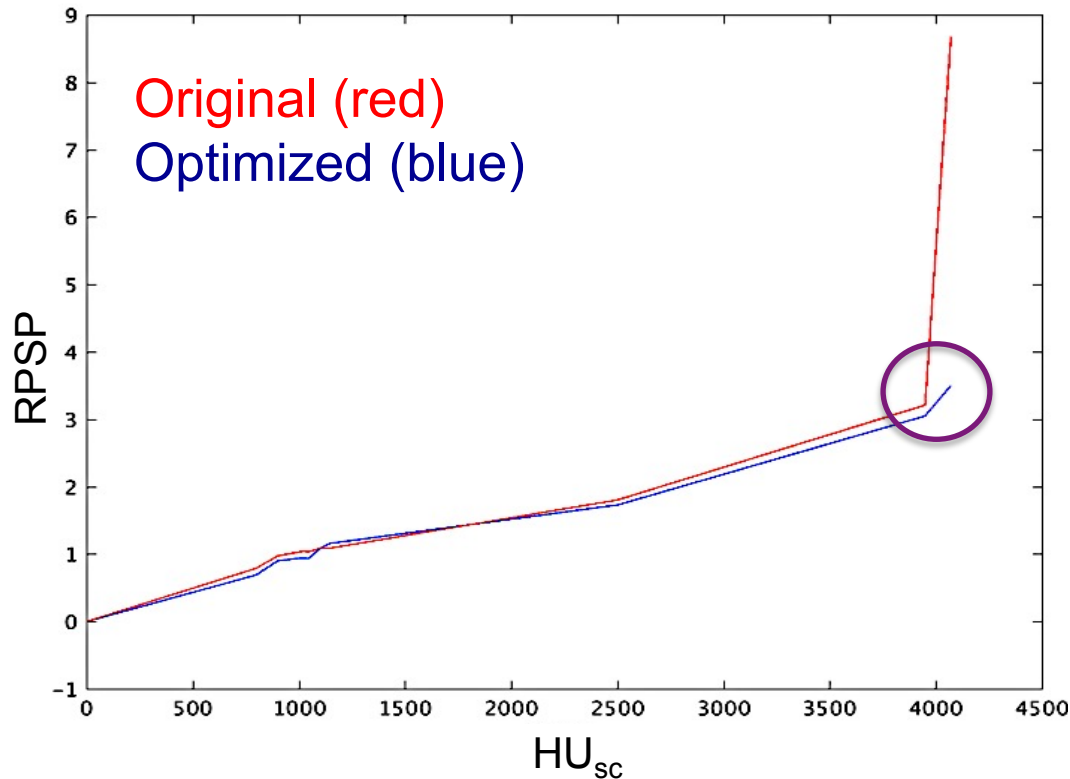
Metric	With PMMA	Without PMMA
RMSE	3.59 mm	2.65 mm
$\chi^2$	5083.80	970.65

## After optimization

Metric	With PMMA	Without PMMA
RMSE	2.36 mm (-34.33%)	1.38 mm (-48.34%)
$\chi^2$	2287.10 (-55.01%)	260.28 (-73.18)



# Original & optimized clinical calibration curves



## Before optimization

- ✧ HU saturates for to  $\sim 4000$  for metals

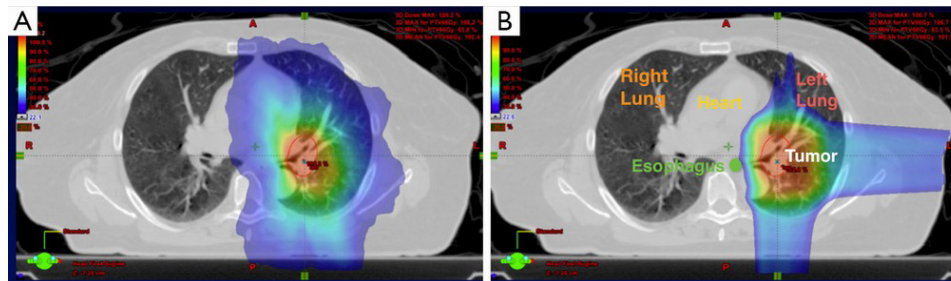
## After optimization

- ✧ No saturation for metals

## Fast and compact detection system with:

- Spatial and angular resolutions
  - Energy resolutions
- Compatible with reconstruction algorithms

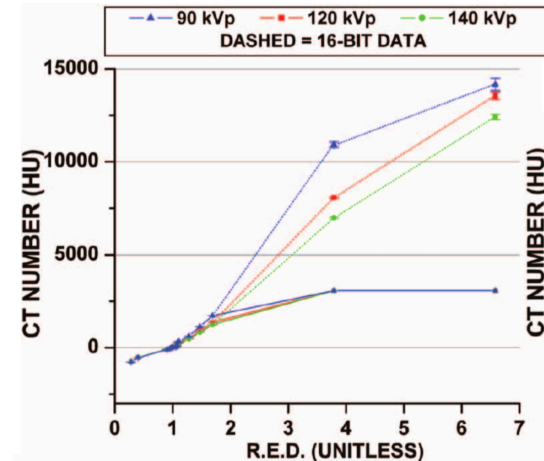
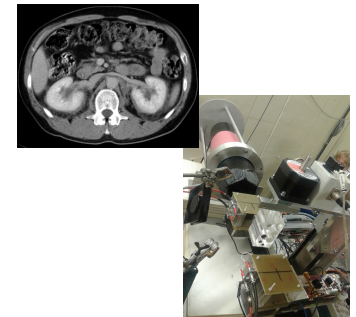
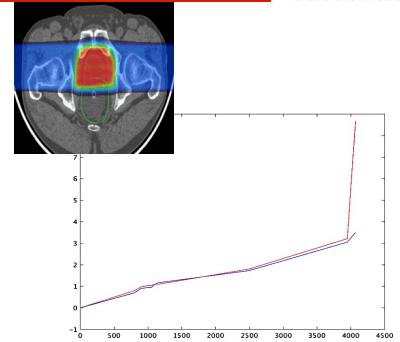
to deliver an accurate map of proton stopping powers of the patient  
to fully benefit from proton therapy



<http://tcr.amegroups.com/article/view/5403/html>

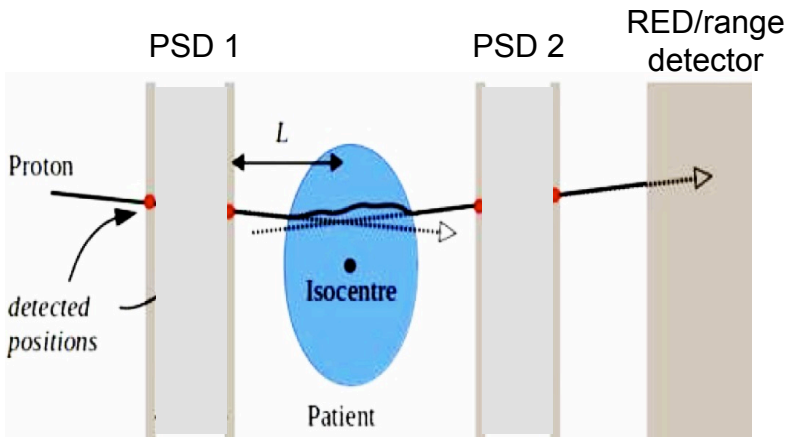
# Future work

- Compare proton treatment plan before / after optimization
- Optimization of the clinical calibration curve:
  - further split of each segments into smaller segments  
→ to account for larger heterogeneities in human tissue
- Include CT/DECT patient data in Geant4 MC pRG simulations
- Validate Geant4 MC simulations with the pRG experimental data
- Using 16 bit CT scanner  
→ to improve HU determinations for metals



Glide-Hurst et al,  
Med Phys 40(6)  
(2013) 061711

# Ideal system with tracking detectors



G. Poludniowski et al., *Br J Radiol* (2015)  
88:20150134

- ✓ Easy to mount on a gantry in proton therapy centers
- ✓ Scan time + reconstruction in a clinic of up to 10 s

All to be clinically acceptable!

## ✓ Tracking detectors

- **Low Z and WET** → minimum MCS in a detector
- **Fast** → high count rate (> MHz), based on Timepix3, time resolution ~ns
- **Spatial resolution** → 50  $\mu\text{m}$
- **Full proton track** determination
- **Modular** → ultimate size 30x30  $\text{cm}^2$

## ✓ Residual energy detector

- **Fast** scintillator (YAG:Ce, LaBr<sub>3</sub>) → **good energy resolution** of up to 1%
- **Fast** → high count rate (> MHz)

## Detection system:

### Position detectors:

- (1) Improved data acquisition for Timepix3 (fast & compact) → **MHz rate**
- (3) Increase the size of the detectors (sufficient in clinics) → **100 x 100 mm<sup>2</sup>**
- (4) 3D information of the proton tract with a good position resolution (good angle reconstruction) → **50 μm**

### Energy:

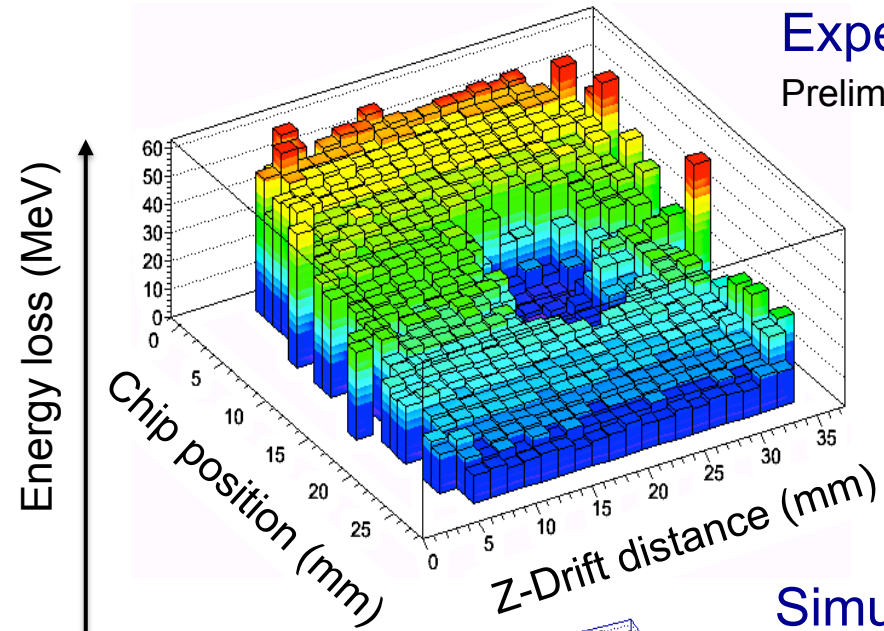
- (1) Fast energy detector → **MHz rate**
- (2) Energy resolution → **≤ 1%**

# Reconstruction of imaged object: trapezoid

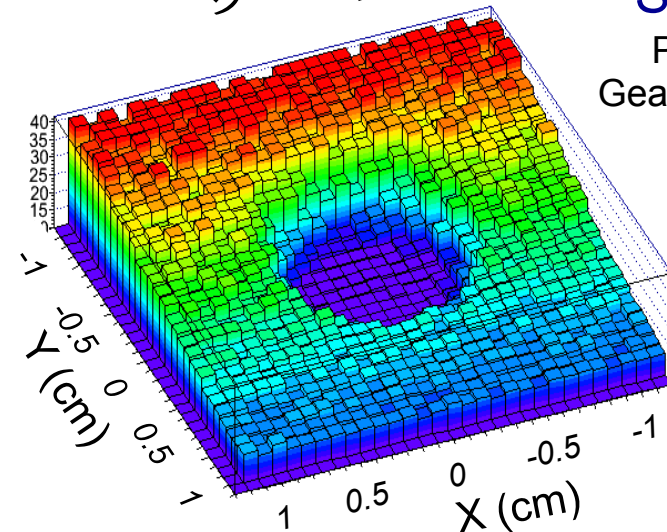
Scattered proton beam  
 of 30 x 30 mm<sup>2</sup> size



Brass trapezoid  $\rho = 8.55 \text{ g/cm}^3$   
 Polymer  $\rho = 1.18 \text{ g/cm}^3$



Experiment  
 Preliminary data

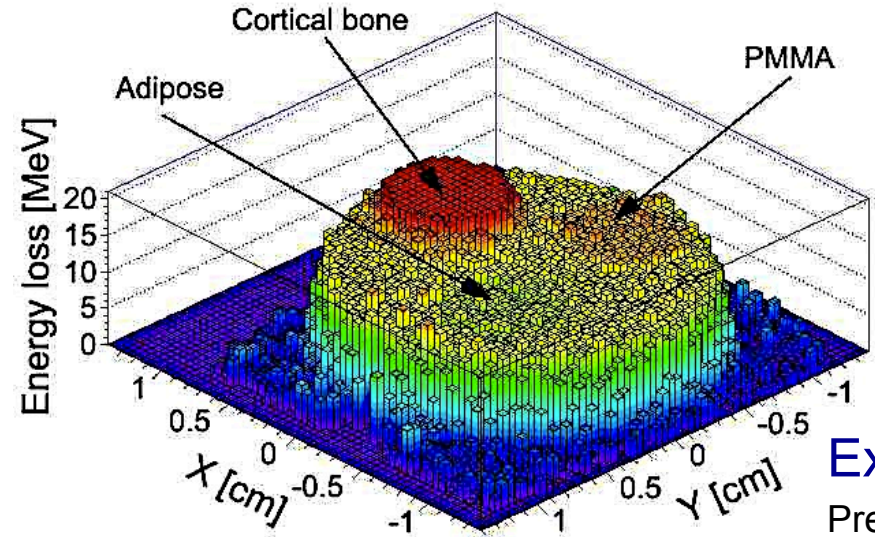
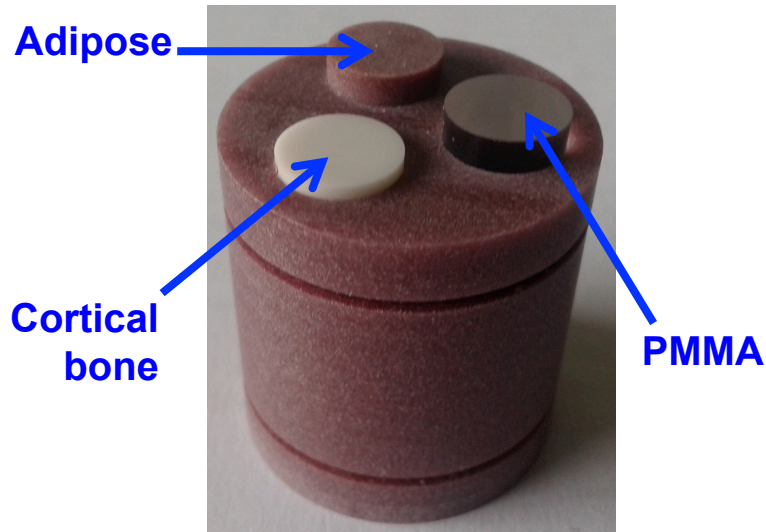


Simulations  
 Performed with  
 Geant4-based MC

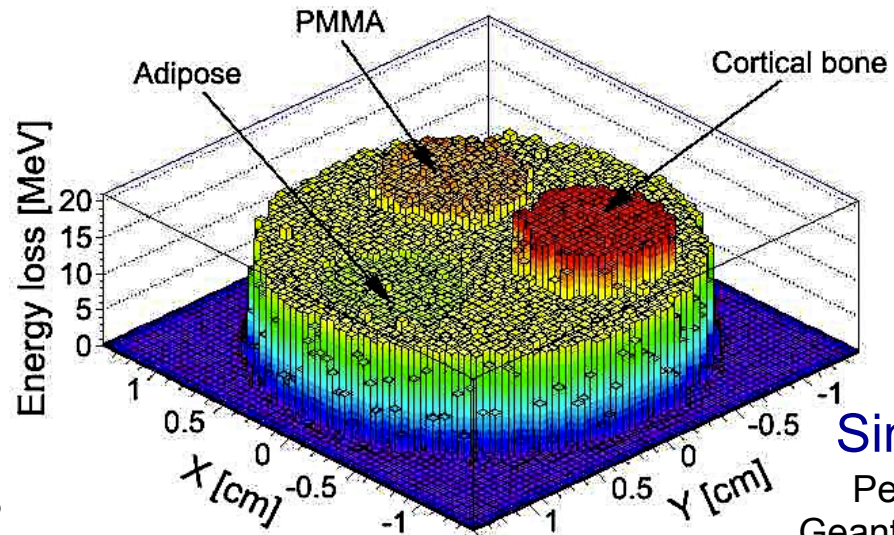


# Reconstruction of object with tissue-like inserts

Scattered proton beam  
of 30 x 30 mm<sup>2</sup> size



**Experiment**  
 Preliminary data



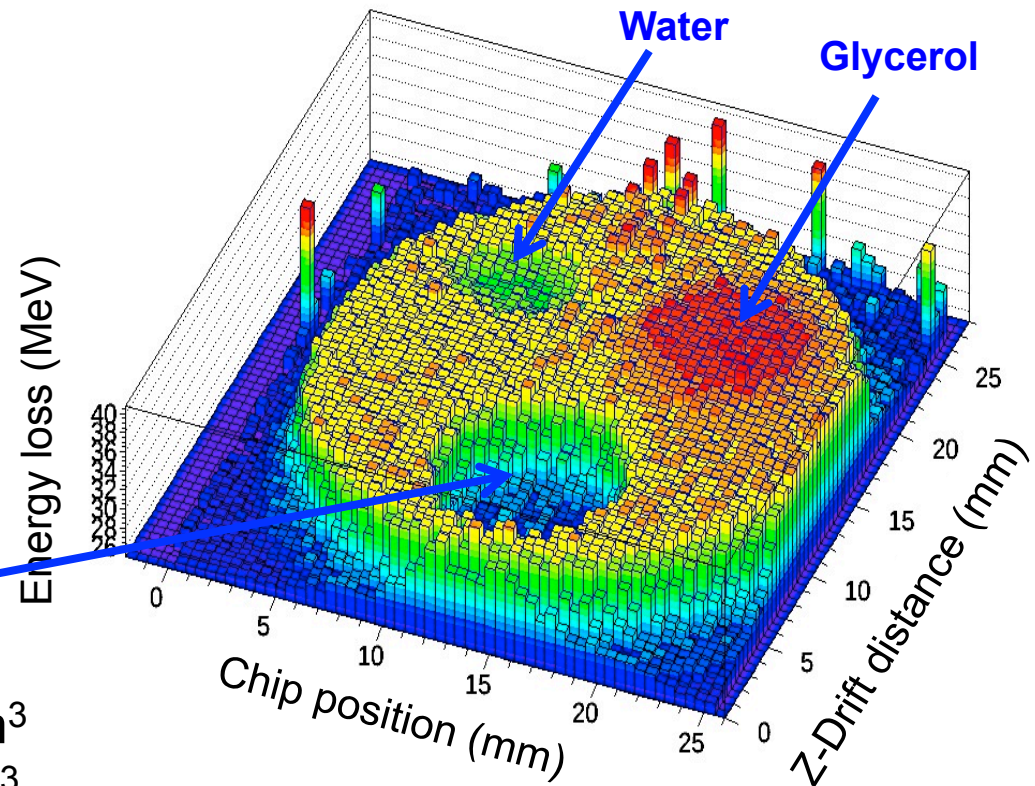
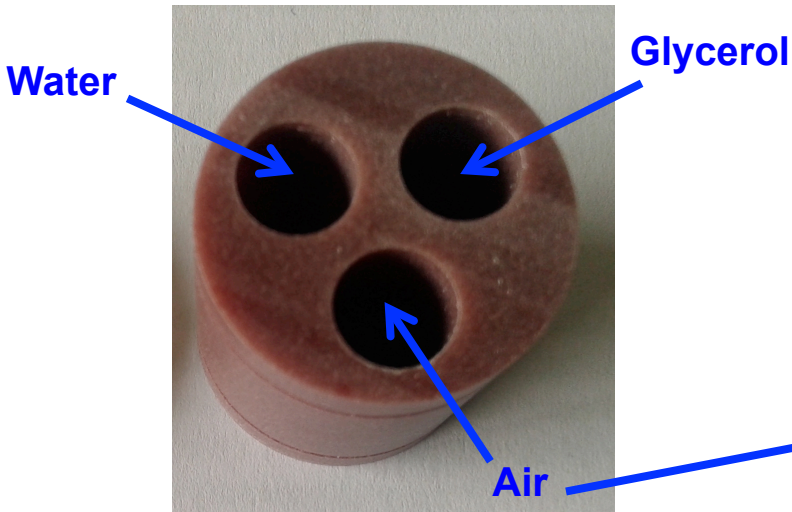
**Simulations**  
 Performed with  
 Geant4-based MC

Adipose (fat)	$\rho = 0.92 \text{ g/cm}^3$
PMMA	$\rho = 1.19 \text{ g/cm}^3$
Cortical bone	$\rho = 1.82 \text{ g/cm}^3$
CT solid water	$\rho = 1.015 \text{ g/cm}^3$

# Reconstruction of object with air and liquid inserts

Experiment  
Preliminary data

Scattered proton beam  
of 30 x 30 mm<sup>2</sup> size



Air	$\rho = 1.29 \cdot 10^{-3}$	g/cm <sup>3</sup>
Water	$\rho = 1.00$	g/cm <sup>3</sup>
Glycerol	$\rho = 1.26$	g/cm <sup>3</sup>
CT solid water	$\rho = 1.015$	g/cm <sup>3</sup>



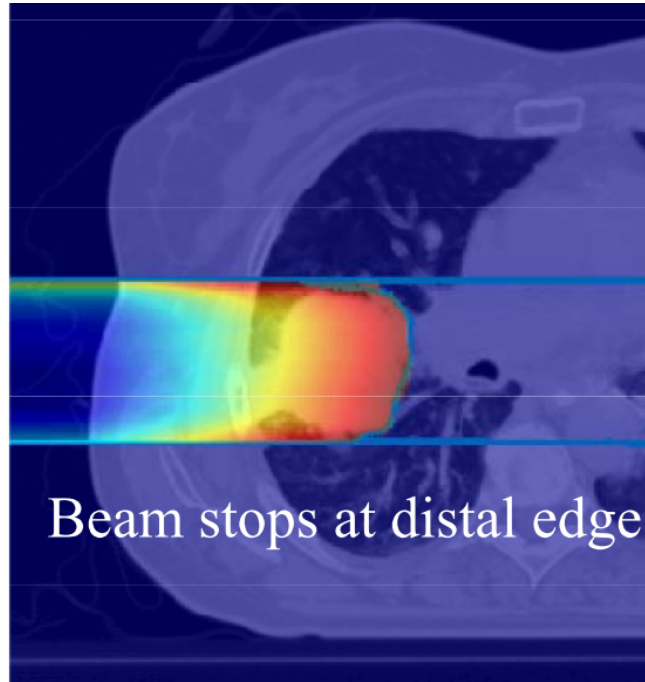
# The AGOR cyclotron

- Superconducting magnet (up to 4.1 T)
- **Protons up to 190 MeV**
- Alpha particles,  **$^{12}\text{C}$  up to 90 MeV/u**
- Heavy ions:  $600 (q/A)^2 \text{ MeV/u}$

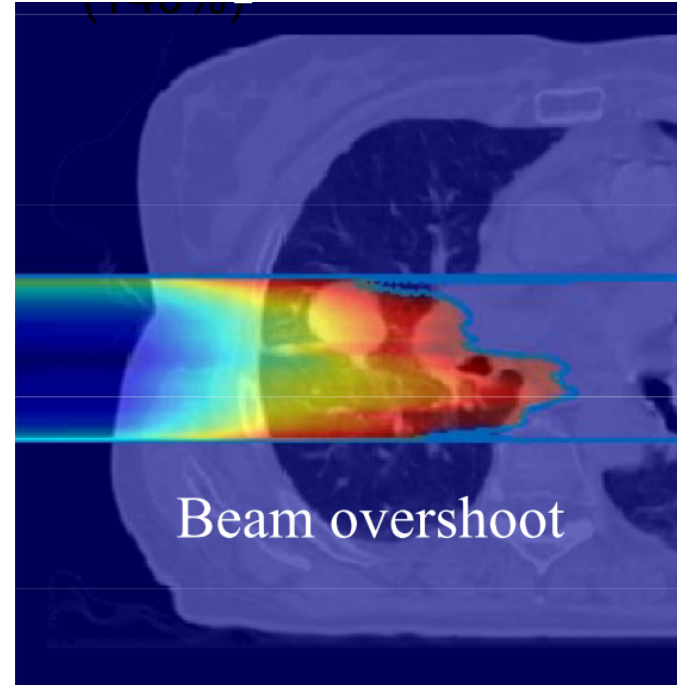


# Tumor modification during treatment: an example

source: S. Mori en G.T.Y Chen, MGH



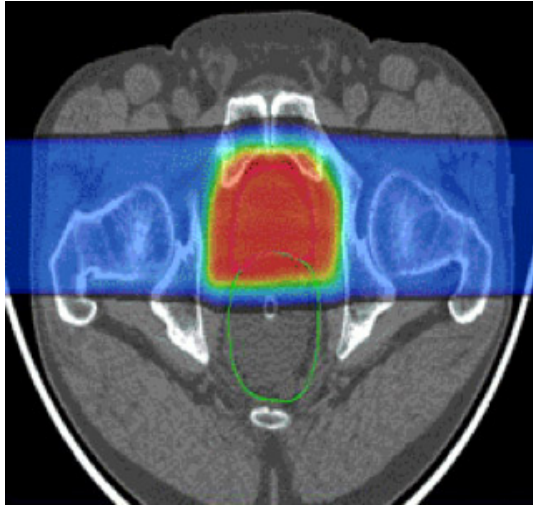
**before treatment**



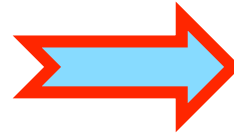
**after 5 weeks**

# Future proton therapy work flow

## Proton Treatment Plan



Scan of a patient  
immediately before  
treatment



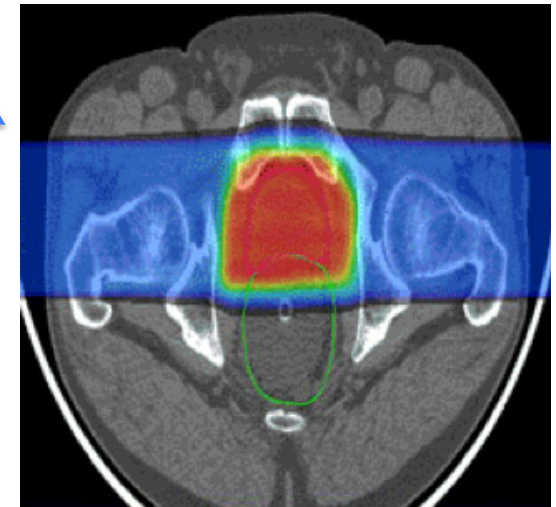
\* Proton radiography/CT

Directly measured  
3D map of proton  
stopping powers

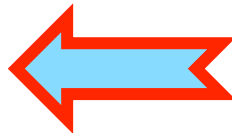
Online  
treatment plan  
adaptation

- \* Accurate ( $< 1\%$ )
- \* Fast (1-10 sec)

Updated  
Proton Treatment Plan



Treatment  
verification



Treatment

